
Not All Data are Good Labels: On the Self-supervised Labeling for Time Series Forecasting

Yuxuan Yang^{1,2}, Dalin Zhang³, Yuxuan Liang⁴, Hua Lu⁵, Gang Chen^{1,2}, Huan Li^{1,2}✉

¹The State Key Laboratory of Blockchain and Data Security, Zhejiang University

²Hangzhou High-Tech Zone (Binjiang) Institute of Blockchain and Data Security

³Space Information Research Institute, Hangzhou Dianzi University

⁴The Hong Kong University of Science and Technology (Guangzhou)

⁵Department of Computer Science, Aalborg university, Denmark

{yangyuxuan, cg, lihuan.cs}@zju.edu.cn

zhangdalin@hdu.edu.cn, yuxliang@outlook.com, luhua@cs.aau.dk

Abstract

Time Series Forecasting (TSF) is a crucial task in various domains, yet existing TSF models rely heavily on high-quality data and insufficiently exploit all available data. This paper explores a novel self-supervised approach to re-label time series datasets by inherently constructing candidate datasets. During the optimization of a simple reconstruction network, intermediates are used as pseudo labels in a self-supervised paradigm, improving generalization for any predictor. We introduce the Self-Correction with Adaptive Mask (SCAM), which discards overfitted components and selectively replaces them with pseudo labels generated from reconstructions. Additionally, we incorporate Spectral Norm Regularization (SNR) to further suppress overfitting from a loss landscape perspective. Our experiments on eleven real-world datasets demonstrate that SCAM consistently improves the performance of various backbone models. This work offers a new perspective on constructing datasets and enhancing the generalization of TSF models through self-supervised learning. The code is available at <https://github.com/SuDIS-ZJU/SCAM>.

1 Introduction

Time Series Forecasting (TSF) is a crucial task with extensive applications in energy, finance, engineering, and many other domains. Recent advances in deep learning have resulted in TSF methods that outperform traditional methods in precision, robustness, and scalability [53, 31, 36].

Nevertheless, deep learning-based TSF methods still face significant challenges such as overfitting, dependence on high-quality datasets, and inconsistent performance across datasets — issues exacerbated by flawed evaluation practices [34, 30]. Central to these challenges is the problem of *low-quality labels*¹, associated with inherent noise and anomalies in raw data. Existing strategies, such as multimodal data integration [43, 4] and dataset scaling [35], focus on augmenting or refining datasets but fail to address the core limitation: the reliance on raw labels as ground truth. To address this, we pose two critical questions:

1. *Can the reliance on high-quality labeled time series datasets be alleviated, given their scarcity?*

¹In TSF, given two adjacent windows in a time series, x (input window) and y (output window), “labels” refer to y fitted by predictions $\hat{y} = f(x; \theta)$ in a supervised learning setting.

2. Can the potential of existing time series datasets be better exploited to improve model performance?

We posit that both answers are positive by redefining how labels are generated. *Instead of treating raw labels as immutable targets, we selectively replace them with “pseudo labels” generated self-supervisedly.*

The key idea is that the pseudo labels can be created from an inherent search through *candidate datasets* created by an auxiliary reconstruction task. In this process, raw labels are partially replaced with reconstructions, guided by an adaptive mask that identifies overfitted raw components and selectively replaces them with pseudo labels for predictions in the supervised setting. This self-supervised learning paradigm significantly enhances the generalization of TSF models compared to traditional supervised learning, which rigidly adheres to raw labels.

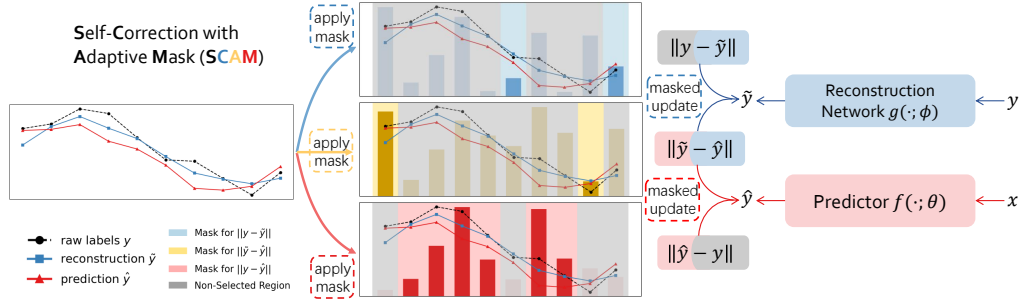


Figure 1: The illustration of the proposed method SCAM.

From an intuitive perspective, a straightforward reconstruction network $g(\cdot; \phi)$ can be employed to generate pseudo-labels in a self-supervised manner. To assess the feasibility of training such a reconstruction network, we conduct an initial evaluation using a grid search algorithm (Section 3.1, Appendix B). The network g is optimized to learn an identity mapping (i.e., reconstruction) of the raw labels over multiple training epochs. During each epoch, the intermediate parameters of g can be frozen to produce an approximate reconstruction of the dataset. Empirical observations reveal that when certain predictors $f(\cdot; \theta)$ are trained from scratch on these intermediate datasets, they exhibit superior performance compared to their counterparts trained exclusively on the raw datasets.

While the reconstruction-based approach demonstrates potential for pseudo-label generation, determining optimal parameters ϕ presents a significant challenge. Specifically, the reconstruction loss (i.e., $\|y - \hat{y}\|$), when combined with the original supervised loss (i.e., $\|\hat{\tilde{y}} - y\|$), tends to drive $g(\cdot; \phi)$ toward reproducing the raw labels. This phenomenon induces an undesirable “overfitting” behavior during training.

To better analyze overfitting, we derive a mask form of the co-objective loss, which partitions original time series into distinct components (see Figure 1). We employ a criterion, namely the *sharpness metric* λ_{max} [10], which detects overfitting by evaluating the sharpness of loss landscape. Using λ_{max} and practical evaluations of the decomposed loss, we identify the overfitted components. This process, termed **Self-Correction with Adaptive Mask** (SCAM), discards raw data labels (y) based on reconstruction results (\hat{y}) and current predictions ($\hat{\tilde{y}}$), smoothing the loss landscape and enhancing the generalization of the predictor model $f(\cdot; \theta)$.

We apply masked updates on a reconstruction network $g(\cdot; \phi)$ and a predictor model $f(\cdot; \theta)$ during training. During inference, the prediction will be generated directly by the updated $f(\cdot; \theta)$ **with no additional cost**. To further generalize across models of varying complexities, we also propose to apply Spectral Norm Regularization [46, 26] to parameters of the first or last linear layers without altering optimizers like previous works [10].

We summarize our contributions as follows:

- **Novel Perspective:** We explore a novel approach of self-enhancing TSF datasets by incorporating an auxiliary reconstruction task into TSF model training.

- **Self-supervised Paradigm:** We propose a self-supervised paradigm that generates pseudo labels from reconstructions and adaptively replaces overfitted raw labels to improve models' generalizability.
- **Detailed Analysis:** We confirm the effectiveness of the proposed self-supervised mask formulation with extensive analyses over various backbones and real-world datasets.

2 Preliminary

2.1 Problem Formulation

Many previous TSF studies adopt a paradigm that learns a direct mapping between two adjacent windows: the history series (*inputs*) and the future series (*labels*). Let the history series (*resp.* future series) be $\{\mathbf{x}_1, \mathbf{x}_2, \dots, \mathbf{x}_N\} = X \in \mathbb{R}^{L \times N}$ (*resp.* $\{\mathbf{y}_1, \mathbf{y}_2, \dots, \mathbf{y}_N\} = Y \in \mathbb{R}^{H \times N}$) with time series length L (*resp.* H) and dataset size (number of segmented windows) N . For simplicity, we formulate the problem in the univariate scenario, as it naturally extends to the multivariate case by treating each variable as an additional dimension.

Definition 1. A typical TSF process is formulated as a supervised-learning problem, i.e., to find $\theta^* = \arg \min_{\theta} \|f(X; \theta) - Y\|$, where a specified metric $\|\cdot\|$ is used to measure errors, typically the ℓ_1 - or ℓ_2 -norm.

When splitting the data into training and test sets, the training set $D_{trn} = \{X_{trn}, Y_{trn}\}$ and the model $f(\cdot; \theta)$ can determine a minimal target error $\mathcal{L}_{tar} = \|f(X_{test}; \theta^*) - Y_{test}\|$ on the test set $D_{test} = \{X_{test}, Y_{test}\}$.

Usually, TSF models struggle on small or noisy datasets. Now, suppose we can obtain additional **candidate datasets** beyond the observed raw dataset; ideally, this would address the issue. In this sense, we assume a family of such candidate datasets $\mathcal{D} = \{D_i\}$, where the optimal candidate dataset D_i^* enables better generalization for a predictor when evaluated by \mathcal{L}_{tar} on the raw test set.

Without constraints, defining such a dataset family can be overly arbitrary. To handle this, we parameterize the family using a neural network $g(X; \phi) = \tilde{X}$, which is trained on a reconstruction loss $\mathcal{L}_{rec} = \|\tilde{X} - X\|$. During an iterative optimization process (e.g., a typical full-batch gradient descent with learning rate η), a candidate dataset D_i is generated at each iteration step i as follows:

$$D_i = \{\tilde{X}_i, \tilde{Y}_i\} = \{\{g(x; \phi_i) \mid x \in X_i\}, \{g(y; \phi_i) \mid y \in Y_i\}\}, \quad (1)$$

$$\phi_i = \phi_0 - \sum_{k=0}^{i-1} \sum_{x \in X_i \cup Y_i} \eta \nabla_{\phi_k} \|g(x; \phi_k) - x\|.$$

This approach shifts the focus from designing models with different inductive biases to identifying candidate datasets that improve a model's generalization. For TSF scenarios where data are often noisy and challenging to clean, replacing raw datasets with such parameterized candidates can lead to more robust performance. To conclude, we formalize the idea as follows.

Hypothesis 1. Given time series data split into $D_{trn} = \{X_{trn}, Y_{trn}\}$ and $D_{test} = \{X_{test}, Y_{test}\}$, and a predictor model $f(\cdot; \theta)$. In a family of training sets $\mathcal{D}_{\phi} = \{D_{trn}^i\}$ parameterized by $g(\cdot; \phi)$ as in Eq. 1, there exist an optimal $D^* = \{\tilde{X}^*, \tilde{Y}^*\} = \{\{g(x_j; \phi^*)\}, \{g(y_j; \phi^*)\}\}$ such that

$$\|f(X_{test}; \theta^*(\phi^*)) - Y_{test}\| \leq \|f(X_{test}; \theta^*(\phi_i)) - Y_{test}\|, \forall \phi_i,$$

where $\theta^*(\phi_i)$ indicates that θ^* is optimized on $D_{trn}^i = \{\tilde{X}_i, \tilde{Y}_i\} = \{\{g(x_j; \phi_i)\}, \{g(y_j; \phi_i)\}\}$.

2.2 Proposed $g(\cdot; \phi)$ for Reconstruction

We proceed to introduce a simple reconstruction network used in subsequent exploration. Similar to a predictor model, the reconstruction network operates in a sequence-to-sequence fashion, learning a function $g(\cdot; \phi)$ that maps raw series Y to reconstructed series \tilde{Y} . Note that reconstruction is applied only to Y , time series datasets are typically generated from a single series using a moving window approach, where X and Y are almost fully overlapped. By skipping reconstruction for X , the predictor model can use raw series as inputs, avoiding *extra* inference costs or potential distribution shifts.

As depicted in Figure 2, the proposed $g(\cdot; \phi)$ comprises four convolutional layers, a cross-layer concatenation for multi-resolution integration, and a lightweight feedforward network (FFN) to decode the reconstructed results. The convolutional layers primarily act as a parameterized smoothing mechanism, similar to techniques for seasonal-trend decomposition [48, 16, 17]. The FFN then mixes information from different positions in a time series to reconstruct each data point using features extracted by convolutional layers (further details in Appendix D). Without introducing extra noise or patch-wise/point-wise masks [27], we directly learn an identity mapping.

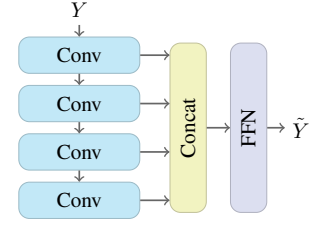


Figure 2: Convolution-FFN reconstruction network.

In essence, $g(\cdot; \phi)$ is designed to traverse diverse alternatives with varying levels of fidelity, which differs in purpose from the usual reconstruction task [22, 24, 18]. Due to this difference, the architecture of $g(\cdot; \phi)$ might benefit from novel designs; however, this is not examined in this study. The proposed $g(\cdot; \phi)$ is merely a simple prototype to validate our ideas and is not claimed superior to other unexplored options for this novel task.

3 Method

3.1 Initial Case

We begin with a simple case where $g(\cdot; \phi)$ evolves from a randomly initialized state toward an approximation of the raw target series Y . This process can be viewed as a *grid search* along the axis of the following reconstruction loss:

$$\ell_{rec} = \|g(y; \phi) - y\|. \quad (2)$$

In this setup, we optimize $g(\cdot; \phi)$ for reconstruction loss using full-batch gradient descent, while the predictor $f(\cdot; \theta)$ is optimized with mini-batch SGD in a vanilla training setting. At each optimization epoch i , we freeze the current parameters of $g(\cdot; \phi_i)$ and generate a candidate dataset D_i . The predictor $f(\cdot; \theta)$ is re-initialized before the epoch and trained on D_i until convergence. The prediction results on the original test set are recorded for each $g(\cdot; \phi_i)$ and corresponding trained $f(\cdot; \theta_i^*)$. A case experiment is conducted on the ETTh1 dataset using a vanilla 2-layer MLP model (for faster and more guaranteed convergence). The pseudo-code for this grid search is provided in Appendix B.

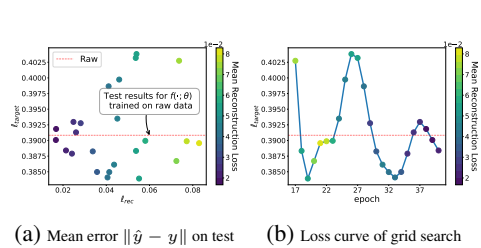


Figure 3: (a) shows the distribution of candidate datasets during the grid search. (b) shows the unsmooth loss curve in grid search. Each scatter in both figures denotes a converged predictor $f(\cdot; \theta)$ on an individual dataset parameterized by $g(\cdot; \phi_i)$.

So far, we can construct a series of candidate datasets $\{D_i\}$ through a two-step optimization process, each easily distinguished by its reconstruction loss, which intuitively measures its similarity to the raw dataset. Evaluating the performance of the same predictor trained on these varying candidate datasets leads to three major observations:

Observation 1 (Improved Labels Enhance Performance). *Figure 3(a) demonstrates the existence of better-labeled candidates which bring better performance for a given predictor, as indicated by the scatter points below the red dotted line — which represents the baseline performance of the predictor trained on the raw dataset.*

Observation 2 (Variable Performance w.r.t. Reconstruction Metric ℓ_{rec}). *A feasible method should evaluate or rank candidate datasets during training without relying on test set performance. However, this remains challenging as datasets with comparable ℓ_{rec} values frequently exhibit substantial differences in actual performance (see Figure 3(a)).*

Observation 3 (Difficult Training). *Training involves an unstable loss curve (Figure 3(b)), meaning many potentially superior candidate datasets (or equivalently $g(\cdot; \phi)$) could be missed. Moreover, training is costly. To ensure the predictor converges, ϕ is only updated after θ is fully trained. This renders grid search impractical for more complex models (e.g., PATCHTST and iTRANSFORMER) or larger datasets.*

In the next section, we propose replacing the brute-force grid search algorithm with a *co-objective training* approach that improves training stability and overall performance.

3.2 Co-objective Training

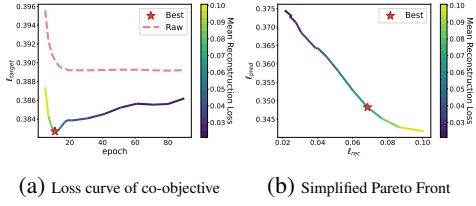


Figure 4: (a) shows the overfitting tendency supported by the increasing ℓ_{target} which measures errors on the test set. (b) shows the Pareto Front of two objectives, tilting top-left indicating the overfitting in (a).

the trajectory of the optimization, rather than its strict optimality, contributes to improved test set performance, the co-objective training can still facilitate the construction of effective candidate datasets.

A single-step optimization using mini-batch SGD would be sufficient, enabling a more smooth trajectory of ϕ during updates (Figure 5(b) vs 5(a) and Figure 4(a) vs Figure 3(b)). Moreover, enabling gradient computation of $\ell_{pred} = \|\tilde{y} - \hat{y}\|$ w.r.t. ϕ introduces a regularization effect, making \tilde{y} updated more cautiously towards y . This allows us to constrain the update of candidate datasets (now specifically represented by the reconstructed \tilde{y}) by jointly constraining gradients w.r.t. both θ and ϕ :

$$\begin{aligned} & \underset{\theta, \phi}{\text{minimize}} && \mathcal{L} = \|\tilde{y} - y\| + \|\tilde{y} - \hat{y}\| \\ & \text{subject to} && \tilde{y} = g(y; \phi), \quad \hat{y} = f(x; \theta), \\ & && \|\nabla_{\theta, \phi} \tilde{y}_i\| \leq \delta, \quad \forall \tilde{y}_i \in \tilde{Y} \end{aligned} \quad (3)$$

where ϕ is trained using both loss terms whereas θ is trained solely on $\ell_{pred} = \|\tilde{y} - \hat{y}\|$. A gradient constraint δ is added to ensure a *smooth* trajectory of \tilde{y} , enabling the co-objective to traverse potential candidate datasets more carefully.

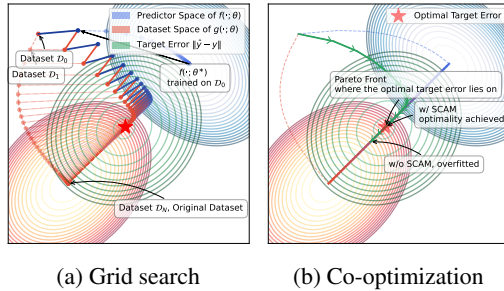


Figure 5: Illustrations of grid search and co-optimization.

Figure 4(a)). Overfitting is a fundamental issue in machine learning, tied to the generalizability of models. In this specific case, this issue arises as the reconstructed dataset gradually approaches the raw dataset, causing the target loss to converge to those of the raw dataset. Similar to the two-step grid search, determining a *reasonable threshold* to identify optimal parameters remains a challenge.

The grid search (Section 3.1) is framed as a two-step optimization process with two distinct objectives involved in finding optimal candidate datasets. The reconstruction optimization primarily provides a trajectory of parameters ϕ_i , without emphasizing optimality. In contrast, the prediction optimization evaluates the predictor’s actual performance.

Our analysis of grid search results suggests that simplifying the training process into a **co-objective optimization** would be beneficial. Since the solution of two-step optimization (though not optimal on the test set) essentially lies on the Pareto Front of the corresponding co-objective optimization (see Figure 4(b)), a natural approach is to search along this front. Again,

The gradient constraint has a surrogate $\|\nabla_{\theta} f\|$ and practically implemented by Spectral Norm Regularization (SNR), as discussed in Section 3.4 and Appendix C. For simplicity, we temporarily omit this constraint, as a 2-layer MLP converges quickly with a small $\|\nabla_{\theta} f\|$. Using the same setting as the grid search, we evaluate the revised loss function for co-optimizing the predictor and the reconstruction network. Figure 4 shows that this co-training improves ℓ_{target} loss while simplifying the two-step training process, leading to more stable optimization and reduced training costs.

However, as the co-training process progresses, it becomes increasingly prone to overfitting (see

To address this specific overfitting issue, we propose solutions summarized in two main components of our method: Self-Correction with Adaptive Mask (SCAM) in Section 3.3 and Spectral Norm Regularization (SNR) in Section 3.4.

3.3 Self-Correction with Adaptive Mask (SCAM)

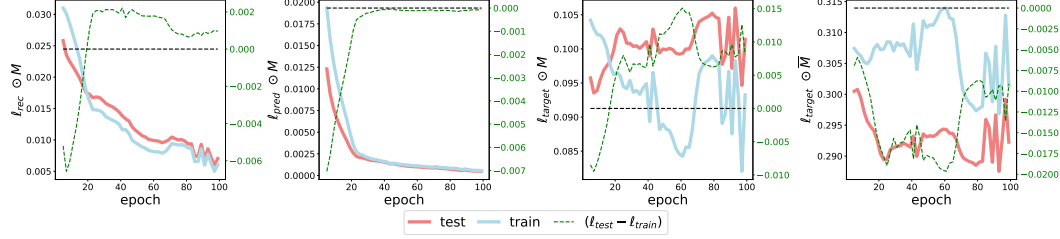


Figure 6: Loss curves of 4 parts divided by the adaptive mask. From left to right, $2|\tilde{y} - y| \odot \overline{M}_{<} \odot M$, $2|\tilde{y} - \hat{y}| \odot M_{<} \odot M$, $|y - \hat{y}| \odot M$ and $|y - \hat{y}| \odot \overline{M}$. The four parts combined are the loss \mathcal{L} in Eq. 4. M refers to the mask where $m_i > 0$ and \overline{M} refers to the mask where $m_i < 0$. The right y-axis (in green) indicates the value for $(\ell_{test} - \ell_{train})$, the differences in losses measured on the test set and the train set. Values (on right y-axis) above 0 (the black dotted line) indicate overfitting.

Mask Form of Self-supervised Loss. In a traditional supervised-learning paradigm, the target loss $\ell_{target} = \|\hat{y} - y\|$ is used only to train a model, implying that all data points are equally treated as valid labels. However, in our approach, where predictors are trained alongside a search for candidate datasets guided by the reconstruction loss, the labels perceived by the predictors are adaptively shifted. Specifically, $\hat{y} = f(x; \theta)$ is trained to fit \tilde{y} , meaning only the second term is optimized for the predictor $f(\cdot; \theta)$ (Eq. 3). The reconstruction loss term, on the other hand, is optimized to provide self-supervised labels for the predictor. We frame this as a self-supervised-learning paradigm that *adaptively* adjusts labels in TSF problems. By comparing the revised loss with the traditional supervised loss, we can explicitly separate the auxiliary loss from the supervised loss: When revisiting the objective \mathcal{L} in co-training, the additional loss term \mathcal{L}_{aux} does not directly contribute to the target objective. Instead, this term depends on the relative positions of \hat{y} , \tilde{y} and y . When the reconstructed \tilde{y} is viewed as a *correction of labels*, \mathcal{L}_{aux} indicates where the correction should be placed. Time series are naturally sparse in real scenarios, often containing spiking signals due to irregular events or anomalies. \mathcal{L}_{aux} encourages the reconstructed \tilde{y} to lie between the prediction \hat{y} and the actual labels y , which can undermine sparsity when used as labels.

$$\begin{aligned}
\mathcal{L} &= \underbrace{|y - \hat{y}|}_{\mathcal{L}_{sup}} + \underbrace{(|\tilde{y} - \hat{y}| + |\tilde{y} - y| - |y - \hat{y}|)}_{\mathcal{L}_{aux}} \\
&\text{Let } A = \tilde{y} - \hat{y}, B = \tilde{y} - y, \\
\mathcal{L} &= \mathcal{L}_{sup} + (|A| + |B| - |A - B|) \\
&= \mathcal{L}_{sup} + \begin{cases} 2 \min\{|A|, |B|\}, & \text{if } AB > 0, \\ 0, & \text{if } AB \leq 0 \end{cases} \quad (4) \\
&\text{Let } m = (\tilde{y} - \hat{y})(\tilde{y} - y), \\
\mathcal{L} &= \mathcal{L}_{sup} + \begin{cases} 2 \min\{|\tilde{y} - \hat{y}|, |\tilde{y} - y|\}, & \text{if } m > 0, \\ 0, & \text{if } m \leq 0 \end{cases} \\
&= \mathcal{L}_{sup} + 2(|\tilde{y} - \hat{y}| \odot M_{<} + |\tilde{y} - y| \odot \overline{M}_{<}) \odot M.
\end{aligned}$$

Here, M is a binary mask defined by $m = (\tilde{y} - \hat{y})(\tilde{y} - y) > 0$, $M_{<}$ ensures $|\tilde{y} - \hat{y}| < |\tilde{y} - y|$, and $\overline{M}_{<}$ represents its complement.

Decoupling Overfitted Components by Adaptive Masks. From the above derivation, we obtain a mask-based co-training loss, allowing us to analyze the causes of overfitting via the mask. As described for \mathcal{L}_{aux} in Eq. 4, the mask M defines the relative positions of y , \tilde{y} , and \hat{y} . Specifically, M masks ℓ_{pred} and ℓ_{rec} to zero when $m_i = (\tilde{y}_i - \hat{y}_i)(\tilde{y}_i - y_i) < 0$. Similarly, $\ell_{target} = |y - y|$ can

also be divided using this mask. By comparing train/test differences in the divided losses (particularly ℓ_{target} , since ℓ_{pred} and ℓ_{rec} are zero when $m_i < 0$), we identify that overfitting primarily stems from $\ell_{target} \odot M$, as shown in Figure 6.

Further evidence is provided by analyzing the loss landscape. A sharpness metric for optimization, proposed by [10], measures the generalization capability of a model. Specifically, the sharpness metric is defined as $\lambda_{max} = \|\nabla_{\theta}^2 \mathcal{L}\|_2^2$, the largest eigenvalue of the Hessian matrix. A higher λ_{max} indicates a sharper loss landscape, which correlates with a worse generalization or more severe overfitting. By computing this metric on the converged parameters, we observe that $\ell_{target} \odot M$ does exhibit a sharper landscape compared to $\ell_{target} \odot \bar{M}$. To address this, we keep the less sharp part of the \mathcal{L}_{sup} term, i.e., $\mathcal{L}_{sup} \odot \bar{M}$, resulting in the revised loss:

$$\mathcal{L} = \underbrace{\|y - \hat{y}\| \odot \bar{M}}_{\text{masked } \mathcal{L}_{sup}} + 2 \underbrace{(\|\tilde{y} - \hat{y}\| \odot M_{<} + \|\tilde{y} - y\| \odot \bar{M}_{<}) \odot M}_{\mathcal{L}_{aux}}. \quad (5)$$

Training with this revised loss reduces the sharpness of the loss landscape. As shown in Figure 7, this effectively mitigates overfitting in the co-training scenario. This represents the final loss form in our proposed method, termed Self-Correction with Adaptive Mask (SCAM), where the mask M is constructed based on an auxiliary reconstruction task. The adaptive M effectively identifies and removes overfitted components of time series labels, enabling the search for more validated parametric candidate datasets $g(y; \phi_i)$.

3.4 Spectral Norm Regularization (SNR)

Note that we have omitted the gradient constraints in Eq. 3. This term is, in fact, positively correlated with $\nabla_{\theta} f(x; \theta)$ (discussed in Appendix E). This further supports our previous analysis, as we have only tested MLP models, which converge easily with lower $\nabla_{\theta} f$. However, when the predictor is replaced by a *Transformer-based* model, the dominant source of overfitting shifts from ℓ_{target} to ℓ_{pred} . This phenomenon is not unique to our self-supervised learning paradigm. For example, [10] proposed sharpness-aware optimization to address overfitting in supervised settings. While gradient penalties are theoretically effective, they may not be practical for complex models like Transformers, as computing second-order derivatives can significantly hinder optimization.

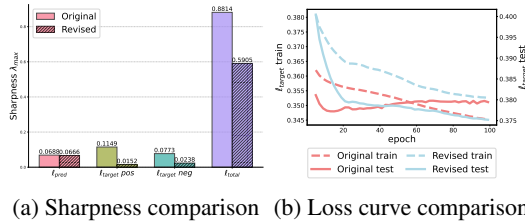


Figure 7: Effectiveness of the revised loss form

siveness of attention score matrices (entropy collapse [49]). Hence, Ilbert et al. [10] conclude that SNR is inapplicable to SA parameters. However, we observe that linear layers — typically the embedding layer before SA and the projection layer after SA — also contribute to the overall sharpness of the loss landscape. Consequently, we propose applying SNR selectively to the pre- and post-SA linear layers. In this way, SNR can work with MLP-based models as they are also composed of multiple linear layers. Further empirical studies on SNR are discussed in Section E.3.

4 Experiment and Analysis

We address three major questions for experiments:

- **Q1:** Is SCAM effective across different backbone models and datasets with varying features?
- **Q2:** How do SCAM and SNR contribute to the potential improvement in model performance?
- **Q3:** How does the self-supervised reconstruction task benefit the predictor models?

Table 1: Performance boost by adding SCAM and SNR to different backbones. Better results are in **bold**.

Models	MLP		+ Ours		CYCLENET		+ Ours		PATCHTST		+ Ours		iTRANS		+ Ours	
Metric	MSE	MAE	MSE	MAE	MSE	MAE	MSE	MAE	MSE	MAE	MSE	MAE	MSE	MAE	MSE	MAE
ETTh1	0.464	0.448	0.437	0.433	0.457	0.441	0.431	0.429	0.469	0.455	0.427	0.433	0.454	0.448	0.431	0.440
ETTh2	0.382	0.405	0.366	0.394	0.388	0.409	0.362	0.393	0.387	0.407	0.370	0.398	0.383	0.407	0.377	0.402
ETTh1	0.391	0.402	0.388	0.398	0.379	0.396	0.368	0.388	0.387	0.400	0.381	0.394	0.407	0.410	0.387	0.399
ETTh2	0.280	0.325	0.276	0.322	0.266	0.341	0.262	0.309	0.281	0.326	0.281	0.326	0.288	0.332	0.283	0.327
Electricity	0.204	0.285	0.203	0.283	0.168	0.259	0.166	0.258	0.205	0.290	0.191	0.275	0.178	0.270	0.173	0.267
Traffic	0.522	0.335	0.494	0.308	0.472	0.301	0.448	0.290	0.481	0.304	0.455	0.288	0.428	0.282	0.411	0.266
Weather	0.262	0.281	0.258	0.278	0.243	0.271	0.242	0.268	0.259	0.281	0.253	0.275	0.258	0.278	0.257	0.278

Our main evaluation involves seven datasets: Electricity, Weather, Traffic, and four ETT datasets (ETTh1, ETTh2, ETTm1, ETTm2), all of which are well-established TSF benchmarks and publicly available [40]. We also test the proposals using four PeMS datasets of a larger scale, as reported in Appendix H. The predictor (i.e., the backbone model integrated with SCAM) covers representative TSF models, including both MLP-based and Transformer-based architectures. MLP [15] is a vanilla 2-layer baseline equipped with RevIN [12] while CYCLENET [17] is a SOTA MLP-based model explicitly capturing cyclic trend in time series. PATCHTST [27] and iTRANSFORMER [21] are Transformer-based models, representing channel-independent and channel-dependent methods, respectively. Following previous settings [53, 40, 41] for direct and fair comparison, we set prediction length $H \in \{96, 192, 336, 720\}$ and look-back length to 96 for all datasets. We provide dataset descriptions, implementation details, and reproduction instructions in Appendix G.

4.1 Main Experiment (Q1)

Table 1 demonstrates consistent performance improvements in all backbones across all datasets when SCAM and SNR are incorporated in the self-supervised-learning paradigm. The full results with detailed breakdowns by prediction lengths are provided in Appendix H. These gains are particularly notable on ETT datasets, which are known for their noisy nature and relatively small size. Notably, Transformer-based models like PATCHTST and iTRANS, which typically underperform compared to lightweight models MLP and CYCLENET on these datasets, show significant enhancements in generalization with SCAM. On the Weather dataset, the boost is more modest, likely due to the intrinsic chaotic nature of atmospheric data.

Regarding **Q1**, our method demonstrates general effectiveness across various backbones and datasets. A well-known discrepancy between MLP-based and Transformer-based models is their dataset preferences: Transformer-based methods excel on large, regular datasets, while MLP-based methods perform better on noisy datasets [30, 34]. SCAM helps bridge this gap by enabling Transformer-based models to perform competitively on traditionally challenging datasets and enhancing the robustness of MLP-based models.

4.2 Ablation Study (Q2)

Table 2: Ablation study for CYCLENET.

+SCAM	+SNR	ETTh1		ETTh2		ETTh1		ETTh2		Weather	
		MSE	MAE	MSE	MAE	MSE	MAE	MSE	MAE	MSE	MAE
\times	\times	0.444	0.436	0.381	0.407	0.379	0.397	0.266	0.313	0.248	0.273
\times	\checkmark	0.438	0.432	0.372	0.398	0.375	0.392	0.265	0.311	0.246	0.272
\checkmark	\times	0.436	0.432	0.365	0.395	0.371	0.390	0.263	0.311	0.242	0.270
\checkmark	\checkmark	0.431	0.429	0.362	0.393	0.368	0.388	0.262	0.309	0.242	0.268

Table 3: Ablation study for iTRANS.

+SCAM	+SNR	ETTh1		ETTh2		ETTh1		ETTh2		Weather	
		MSE	MAE	MSE	MAE	MSE	MAE	MSE	MAE	MSE	MAE
\times	\times	0.438	0.440	0.400	0.417	0.413	0.414	0.299	0.341	0.285	0.306
\times	\checkmark	0.443	0.445	0.399	0.417	0.413	0.415	0.306	0.347	0.283	0.302
\checkmark	\times	0.436	0.438	0.381	0.404	0.391	0.404	0.293	0.342	0.274	0.289
\checkmark	\checkmark	0.431	0.440	0.377	0.402	0.387	0.399	0.283	0.327	0.257	0.278

To answer **Q2**, we present the performance gains from SCAM and SNR through an ablation study (Tables 2 and 3²), using iTRANS (Transformer-based) and CYCLENET (MLP-based) as representatives (the SOTA one in their category).

SNR, a practical alternative to the gradient penalty in Eq. 8, consistently enhances performance across backbones. However, iTRANS, being more prone to overfitting on small datasets (discussed in [10]),

²The results in both tables may have discrepancy in baseline results from Table 1. This is because the Table 1 has baseline results from the original papers, and Table 2 and 3 are from our runs for module modification. See Sec G.3 for further explanations.

benefits less from SNR compared to CYCLENET, likely due to insufficient data for generalization in higher-complexity architectures. With SCAM, both models exhibit significant improvements, leveraging the expanded effective training data.

In summary, SCAM is the primary driver of performance gains, offering consistent and clear improvements. While SNR enhances results as a standalone method, it serves best as a complement to SCAM, acting as an effective surrogate for the gradient penalty in the self-supervised objective.

4.3 SCAM: A Multiple Instance Learning View (Q3)

Multiple Instance Learning (MIL [25, 3]) is a classical weakly-supervised binary classification problem where typically a bag of instances is labeled positive if at least one instance is positive. [8, 5] extend MIL to Time Series Classification by treating an input window as a bag of instances (time points), enabling a model to predict based on instance-level classifications that are more interpretable.

To answer **Q3**, we hypothesize that the effectiveness of SCAM shares similarities with MIL by leveraging instance-level signals, though it does not strictly follow a MIL framework. For a quick illustration, we synthesize a toy dataset where the ground truth is defined as $y = A \sin(\omega_1 x) + B \sin(\omega_2 x)$, with added noise sampled alternately from $\mathcal{N}(0, \sigma_1)$ and $\mathcal{N}(0, \sigma_2)$ in different windows. As shown in Figure 8, when the noise deviation σ is large (left part), SCAM tends to optimize $\ell_{rec} = M \odot \overline{M}_{<} \|\tilde{y} - y\|$, prioritizing robust reconstructions; when σ is small, SCAM shifts focus to optimizing $\ell_{pred} = M \odot M_{<} \|\tilde{y} - y\|$ and $\ell_{target} = \|\hat{y} - y\|$, emphasizing accurate predictions.

This study only reveals a part of SCAM’s self-supervision effectiveness, which is further explored in Appendix E.

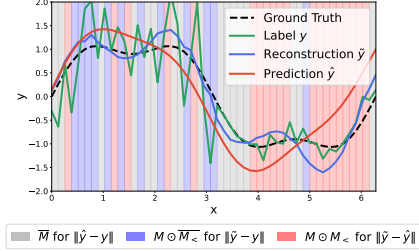


Figure 8: Case study of visualized mask.

5 Related Work

We discuss related techniques from meta-learning and self-supervised learning perspectives, with an inventory of TSF models in Appendix F.

Meta-Learning for Time Series. Meta-Learning, by definition, seeks to perform in a learn-to-learn paradigm. Generally speaking, meta-learning for TSF includes optimization-based and metric-based methods. Optimization-based methods target optimal initial parameters [9], often involving a two-loop optimization process [28, 38]. Metric-based methods [7, 38] learn a metric function that provides more expressive measurements of distances between data samples, commonly comparing training and validation samples.

Our method SCAM aligns with the broader scope of meta-learning. Specifically, the grid search (Section 3.1, Appendix B) follows the two-loop structure similar to optimization-based methods. However, it diverges by focusing on *dataset space* rather than *parameter space*. Additionally, the final mask form of SCAM in essence provides a more accurate metric tailored for a supervised-learning setting. Previous works [38, 7] learn metrics on the sample level (a window of time series), whereas ours focuses on the instance level (individual data points of time series).

Self-supervised Learning for Time Series. Self-supervised learning trains models without relying on manually labeled data by using auxiliary tasks like generation, contrast, and reconstruction to learn expressive representation or create pseudo labels. In the realm of time series, this approach is discussed more in Time Series Classification (TSC) [11, 42, 22]. Recent works [8, 5] present a novel perspective that instances in time series/segments can have multiple labels. They propose corresponding weakly-supervised-learning methods that significantly improve both performance and interpretability.

In this work, we integrate the *multiple-label* perspective by employing an auxiliary reconstruction task, commonly used in TSC, to enhance the performance of TSF. The pseudo labels, often discussed in TSC, are derived from existing, manual ones, while ours are created in a self-supervised paradigm.

6 Conclusion and Future Work

This paper presents a self-supervised approach SCAM that enhances TSF models by selectively replacing overfitted components with pseudo labels derived from intermediate reconstructions. When combined with Spectral Norm Regularization, SCAM improves generalization and robustness across TSF models. Future work will explore extending SCAM to tasks such as time series outlier detection and error correction.

7 Acknowledgment

This work was supported by the National Natural Science Foundation of China (Nos. 62402420, 62402414), Fundamental Research Funds for Central Universities (Grant No. 226202400109), the Zhejiang Provincial Natural Science Foundation (No. LD24F020015), and the National Regional Innovation and Development Joint Fund (No. U24A20254). Huan Li is the corresponding author of this paper.

References

- [1] Md Atik Ahamed and Qiang Cheng. Timemachine: A time series is worth 4 mambas for long-term forecasting. In *ECAI 2024: 27th European Conference on Artificial Intelligence, 19-24 October 2024, Santiago de Compostela, Spain-Including 13th Conference on Prestigious Applications of Intelligent Systems. European Conference on Artificial Intelli*, volume 392, page 1688, 2024.
- [2] Abdul Fatir Ansari, Lorenzo Stella, Caner Turkmen, Xiyuan Zhang, Pedro Mercado, Huibin Shen, Oleksandr Shchur, Syama Sundar Rangapuram, Sebastian Pineda Arango, Shubham Kapoor, et al. Chronos: Learning the language of time series. *arXiv preprint arXiv:2403.07815*, 2024.
- [3] Marc-André Carbonneau, Veronika Cheplygina, Eric Granger, and Ghyslain Gagnon. Multiple instance learning: A survey of problem characteristics and applications. *Pattern recognition*, 77: 329–353, 2018.
- [4] Mouxiang Chen, Lefei Shen, Zhuo Li, Xiaoyun Joy Wang, Jianling Sun, and Chenghao Liu. Visions: Visual masked autoencoders are free-lunch zero-shot time series forecasters. *arXiv preprint arXiv:2408.17253*, 2024.
- [5] Xiwen Chen, Peijie Qiu, Wenhui Zhu, Huayu Li, Hao Wang, Aristeidis Sotiras, Yalin Wang, and Abolfazl Razi. Timemil: Advancing multivariate time series classification via a time-aware multiple instance learning. In *Forty-first International Conference on Machine Learning*, 2024.
- [6] Abhimanyu Das, Weihao Kong, Rajat Sen, and Yichen Zhou. A decoder-only foundation model for time-series forecasting. In *Forty-first International Conference on Machine Learning*, 2024.
- [7] Yuntao Du, Jindong Wang, Wenjie Feng, Sinno Pan, Tao Qin, Renjun Xu, and Chongjun Wang. Adarnn: Adaptive learning and forecasting of time series. In *Proceedings of the 30th ACM international conference on information & knowledge management*, pages 402–411, 2021.
- [8] Joseph Early, Gavin Cheung, Kurt Cutajar, Hanting Xie, Jas Kandola, and Niall Twomey. Inherently interpretable time series classification via multiple instance learning. In *The Twelfth International Conference on Learning Representations*, 2024.
- [9] Chelsea Finn, Pieter Abbeel, and Sergey Levine. Model-agnostic meta-learning for fast adaptation of deep networks. In *International conference on machine learning*, pages 1126–1135. PMLR, 2017.
- [10] Romain Ilbert, Ambroise Odonnat, Vasilii Feofanov, Aladin Virmaux, Giuseppe Paolo, Themis Palpanas, and Ievgen Redko. Samformer: Unlocking the potential of transformers in time series forecasting with sharpness-aware minimization and channel-wise attention. In *Forty-first International Conference on Machine Learning*, 2024.
- [11] Shayan Jawed, Josif Grabocka, and Lars Schmidt-Thieme. Self-supervised learning for semi-supervised time series classification. In *Advances in Knowledge Discovery and Data Mining: 24th Pacific-Asia Conference, PAKDD 2020, Singapore, May 11–14, 2020, Proceedings, Part I* 24, pages 499–511. Springer, 2020.
- [12] Taesung Kim, Jinhee Kim, Yunwon Tae, Cheonbok Park, Jang-Ho Choi, and Jaegul Choo. Reversible instance normalization for accurate time-series forecasting against distribution shift. In *International Conference on Learning Representations*, 2021.
- [13] Diederik P Kingma. Adam: A method for stochastic optimization. *arXiv preprint arXiv:1412.6980*, 2014.
- [14] Seunghan Lee, Taeyoung Park, and Kibok Lee. Learning to embed time series patches independently. *arXiv preprint arXiv:2312.16427*, 2023.
- [15] Zhe Li, Shiyi Qi, Yiduo Li, and Zenglin Xu. Revisiting long-term time series forecasting: An investigation on linear mapping. *arXiv preprint arXiv:2305.10721*, 2023.

- [16] Shengsheng Lin, Weiwei Lin, Wentai Wu, Haojun Chen, and Junjie Yang. Sparsetsf: Modeling long-term time series forecasting with* 1k* parameters. In *Forty-first International Conference on Machine Learning*, 2024.
- [17] Shengsheng Lin, Weiwei Lin, HU Xinyi, Wentai Wu, Ruichao Mo, and Haocheng Zhong. Cyclenet: Enhancing time series forecasting through modeling periodic patterns. In *The Thirty-eighth Annual Conference on Neural Information Processing Systems*, 2024.
- [18] Jiexi Liu and Songcan Chen. Timesurl: Self-supervised contrastive learning for universal time series representation learning. In *Proceedings of the AAAI Conference on Artificial Intelligence*, volume 38, pages 13918–13926, 2024.
- [19] Xu Liu, Junfeng Hu, Yuan Li, Shizhe Diao, Yuxuan Liang, Bryan Hooi, and Roger Zimmermann. Unitime: A language-empowered unified model for cross-domain time series forecasting. In *Proceedings of the ACM on Web Conference 2024*, 2024.
- [20] Yong Liu, Haixu Wu, Jianmin Wang, and Mingsheng Long. Non-stationary transformers: Exploring the stationarity in time series forecasting. *Advances in Neural Information Processing Systems*, 35:9881–9893, 2022.
- [21] Yong Liu, Tengge Hu, Haoran Zhang, Haixu Wu, Shiyu Wang, Lintao Ma, and Mingsheng Long. itransformer: Inverted transformers are effective for time series forecasting. In *The Twelfth International Conference on Learning Representations*, 2024.
- [22] Ziyu Liu, Azadeh Alavi, Minyi Li, and Xiang Zhang. Self-supervised learning for time series: Contrastive or generative? *arXiv preprint arXiv:2403.09809*, 2024.
- [23] Donghao Luo and Xue Wang. Modernrctn: A modern pure convolution structure for general time series analysis. In *The Twelfth International Conference on Learning Representations*, 2024.
- [24] Yanqing Ma, Carmine Ventre, and Maria Polukarov. Denoised labels for financial time series data via self-supervised learning. In *Proceedings of the Third ACM International Conference on AI in Finance*, pages 471–479, 2022.
- [25] Oded Maron and Tomás Lozano-Pérez. A framework for multiple-instance learning. *Advances in neural information processing systems*, 10, 1997.
- [26] Takeru Miyato, Toshiki Kataoka, Masanori Koyama, and Yuichi Yoshida. Spectral normalization for generative adversarial networks. In *International Conference on Learning Representations*, 2018.
- [27] Yuqi Nie, Nam H Nguyen, Phanwadee Sinthong, and Jayant Kalagnanam. A time series is worth 64 words: Long-term forecasting with transformers. *arXiv preprint arXiv:2211.14730*, 2022.
- [28] Boris N Oreshkin, Dmitri Carpov, Nicolas Chapados, and Yoshua Bengio. Meta-learning framework with applications to zero-shot time-series forecasting. In *Proceedings of the AAAI conference on artificial intelligence*, volume 35, pages 9242–9250, 2021.
- [29] Adam Paszke, Sam Gross, Francisco Massa, Adam Lerer, James Bradbury, Gregory Chanan, Trevor Killeen, Zeming Lin, Natalia Gimelshein, Luca Antiga, et al. Pytorch: An imperative style, high-performance deep learning library. *Advances in neural information processing systems*, 32, 2019.
- [30] Xiangfei Qiu, Jilin Hu, Lekui Zhou, Xingjian Wu, Junyang Du, Buang Zhang, Chenjuan Guo, Aoying Zhou, Christian S Jensen, Zhenli Sheng, et al. Tfb: Towards comprehensive and fair benchmarking of time series forecasting methods. *arXiv preprint arXiv:2403.20150*, 2024.
- [31] David Salinas, Valentin Flunkert, Jan Gasthaus, and Tim Januschowski. Deepar: Probabilistic forecasting with autoregressive recurrent networks. *International journal of forecasting*, 36(3): 1181–1191, 2020.
- [32] John Schulman. Trust region policy optimization. *arXiv preprint arXiv:1502.05477*, 2015.

- [33] John Schulman, Filip Wolski, Prafulla Dhariwal, Alec Radford, and Oleg Klimov. Proximal policy optimization algorithms. *arXiv preprint arXiv:1707.06347*, 2017.
- [34] Zezhi Shao, Fei Wang, Yongjun Xu, Wei Wei, Chengqing Yu, Zhao Zhang, Di Yao, Tao Sun, Guangyin Jin, Xin Cao, et al. Exploring progress in multivariate time series forecasting: Comprehensive benchmarking and heterogeneity analysis. *IEEE Transactions on Knowledge and Data Engineering*, 2024.
- [35] Jingzhe Shi, Qinwei Ma, Huan Ma, and Lei Li. Scaling law for time series forecasting. *arXiv preprint arXiv:2405.15124*, 2024.
- [36] Sean J Taylor and Benjamin Letham. Forecasting at scale. *The American Statistician*, 72(1): 37–45, 2018.
- [37] Xue Wang, Tian Zhou, Qingsong Wen, Jinyang Gao, Bolin Ding, and Rong Jin. Card: Channel aligned robust blend transformer for time series forecasting. In *The Twelfth International Conference on Learning Representations*, 2024.
- [38] Gerald Woo, Chenghao Liu, Doyen Sahoo, Akshat Kumar, and Steven Hoi. Deeptime: Deep time-index meta-learning for non-stationary time-series forecasting. 2022.
- [39] Gerald Woo, Chenghao Liu, Akshat Kumar, Caiming Xiong, Silvio Savarese, and Doyen Sahoo. Unified training of universal time series forecasting transformers. 2024.
- [40] Haixu Wu, Jiehui Xu, Jianmin Wang, and Mingsheng Long. Autoformer: Decomposition transformers with auto-correlation for long-term series forecasting. *Advances in neural information processing systems*, 2021.
- [41] Haixu Wu, Tengge Hu, Yong Liu, Hang Zhou, Jianmin Wang, and Mingsheng Long. Timesnet: Temporal 2d-variation modeling for general time series analysis. In *The Eleventh International Conference on Learning Representations*, 2023.
- [42] Liang Xi, Zichao Yun, Han Liu, Ruidong Wang, Xunhua Huang, and Haoyi Fan. Semi-supervised time series classification model with self-supervised learning. *Engineering Applications of Artificial Intelligence*, 116:105331, 2022.
- [43] Zhijian Xu, Yuxuan Bian, Jianyuan Zhong, Xiangyu Wen, and Qiang Xu. Beyond trend and periodicity: Guiding time series forecasting with textual cues. *arXiv preprint arXiv:2405.13522*, 2024.
- [44] Zhijian Xu, Ailing Zeng, and Qiang Xu. Fits: Modeling time series with 10k parameters. In *The Twelfth International Conference on Learning Representations*, 2024.
- [45] Kun Yi, Qi Zhang, Wei Fan, Shoujin Wang, Pengyang Wang, Hui He, Ning An, Defu Lian, Longbing Cao, and Zhendong Niu. Frequency-domain mlps are more effective learners in time series forecasting. *Advances in Neural Information Processing Systems*, 36, 2024.
- [46] Yuichi Yoshida and Takeru Miyato. Spectral norm regularization for improving the generalizability of deep learning. *arXiv preprint arXiv:1705.10941*, 2017.
- [47] Chengqing Yu, Fei Wang, Zezhi Shao, Tao Sun, Lin Wu, and Yongjun Xu. Dsformer: A double sampling transformer for multivariate time series long-term prediction. In *Proceedings of the 32nd ACM international conference on information and knowledge management*, pages 3062–3072, 2023.
- [48] Ailing Zeng, Muxi Chen, Lei Zhang, and Qiang Xu. Are transformers effective for time series forecasting? In *Proceedings of the AAAI conference on artificial intelligence*, volume 37, pages 11121–11128, 2023.
- [49] Shuangfei Zhai, Tatiana Likhomanenko, Etai Littwin, Dan Busbridge, Jason Ramapuram, Yizhe Zhang, Jiatao Gu, and Joshua M Susskind. Stabilizing transformer training by preventing attention entropy collapse. In *International Conference on Machine Learning*, pages 40770–40803. PMLR, 2023.

- [50] Yitian Zhang, Liheng Ma, Soumyasundar Pal, Yingxue Zhang, and Mark Coates. Multi-resolution time-series transformer for long-term forecasting. In *International Conference on Artificial Intelligence and Statistics*. PMLR, 2024.
- [51] Yunhao Zhang and Junchi Yan. Crossformer: Transformer utilizing cross-dimension dependency for multivariate time series forecasting. In *The Eleventh International Conference on Learning Representations*, 2023.
- [52] Lifan Zhao and Yanyan Shen. Rethinking channel dependence for multivariate time series forecasting: Learning from leading indicators. In *The Twelfth International Conference on Learning Representations*, 2024.
- [53] Haoyi Zhou, Shanghang Zhang, Jieqi Peng, Shuai Zhang, Jianxin Li, Hui Xiong, and Wancai Zhang. Informer: Beyond efficient transformer for long sequence time-series forecasting. In *Proceedings of the AAAI conference on artificial intelligence*, 2021.
- [54] Tian Zhou, Ziqing Ma, Qingsong Wen, Xue Wang, Liang Sun, and Rong Jin. Fedformer: Frequency enhanced decomposed transformer for long-term series forecasting. In *International conference on machine learning*, pages 27268–27286. PMLR, 2022.

A Limitations

Our work constrains the discussion for TSF models in MLP- and Transformer-based ones, excluding other potentially feasible solutions [23, 1]. We omit these newly explored architectures since they have not outperformed the baseline methods we have adopted under the same budget. Also, we have not verified our method on LLM-based models (or models of an LLM-level scale) [39, 2] due to the excessive costs required.

B Grid Search Algorithm in Initial Case

In Section 3.1, we have introduced the grid search process to illustrate how the reconstruction network $g(\cdot; \phi)$ evolves to approximate the raw target series Y by minimizing the reconstruction loss $\ell_{rec} = \|g(y; \phi) - y\|$. The following Algorithm 1 provides a detailed implementation of this process, where the reconstruction network $g(\cdot; \phi)$ and the predictor model $f(\cdot; \theta)$ are jointly optimized to minimize both reconstruction and prediction losses. Specifically, for each candidate reconstruction parameter ϕ_i (line 1), the predictor’s parameters θ and its optimizer are initialized (line 2). In the inner loop (line 3), the predictor is optimized by first reconstructing \tilde{y}_i using $g(\cdot; \phi_i)$ (line 6), then calculating the prediction loss ℓ_{pred} (line 7) and reconstruction loss ℓ_{rec} (line 8). The prediction loss ℓ_{pred} is backpropagated to update θ (line 8), and this process repeats until the gradient ∇_{θ} falls below a threshold α or the maximum steps J are reached (line 3). After optimizing θ , the reconstruction loss ℓ_{rec} is backpropagated to update ϕ (line 11), and this process is repeated for all N candidates to find the best ϕ (line 1).

Algorithm 1 Grid Search along ℓ_{rec}

Parameters : ϕ w.r.t reconstruction network $g(\cdot; \phi)$;
 θ w.r.t predictor model $f(\cdot; \theta)$
Optimizers : Opt_{ϕ} w.r.t ϕ (outer loop);
 Opt_{θ} w.r.t θ (inner loop)
Initialize : ϕ, Opt_{ϕ}

```

1 for  $i \leftarrow 0$  to  $N$  do
  ▷  $N$  for number of candidates
2   Initialize  $\theta, Opt_{\theta}$ ;  $j \leftarrow 0$ 
3   while  $\nabla_{\theta} > \alpha$  and  $j \leq J$  do
    ▷  $J$  for maximum steps to optimize a predictor
4      $\ell_{rec} \leftarrow 0$ 
5     foreach  $(x, y) \in (X, Y)$  do
6        $\tilde{y}_i \leftarrow g(y; \phi_i)$ 
7        $\ell_{pred} \leftarrow \|f(x; \theta) - \tilde{y}_i\|$ 
8        $\ell_{rec} \leftarrow \ell_{rec} + \|\tilde{y}_i - y\|$ 
9       Backpropagate  $\ell_{pred}$  and update  $\theta$  using  $Opt_{\theta}$ 
10     $j \leftarrow j + 1$ 
11  Backpropagate  $\ell_{rec}$  and update  $\phi$  using  $Opt_{\phi}$ 

```

C Further Discussion on Gradient Constraint

Recall that in Section 3.2, we have proposed the co-training objective as:

$$\begin{aligned}
& \underset{\theta, \phi}{\text{minimize}} && \mathcal{L} = \|\tilde{y} - y\| + \|\tilde{y} - \hat{y}\| \\
& \text{subject to} && \tilde{y} = g(y; \phi), \quad \hat{y} = f(x; \theta), \\
& && \|\nabla_{\theta, \phi} \tilde{y}_i\| \leq \delta, \quad \forall \tilde{y}_i \in \tilde{Y}.
\end{aligned}$$

With constraints on the gradient of \tilde{y} , the co-training update allows for a more stable optimization compared to the grid search using a two-step optimization. When viewing each intermediate ϕ_i as an individual candidate dataset, applying cautious updates to $\tilde{y}_i = g(y; \phi_i)$ introduces additional candidate datasets along the optimization trajectory, enriching the search process.

However, since $\nabla_{\theta, \phi} \tilde{y}_i$ is not practically computable for each \tilde{y}_i within a single step of optimization, we turn to look for a surrogate term to replace this constraint.

Note that

$$\begin{aligned}
\nabla_{\phi, \theta} \tilde{y}_i &= [\nabla_{\phi} g \quad \nabla_{\theta} g] \\
&= \begin{bmatrix} \nabla_{\phi} g & \nabla_{\phi} g \frac{\nabla_{\theta} \mathcal{L}}{\nabla_{\phi} \mathcal{L}} \end{bmatrix} \\
&= \begin{bmatrix} \nabla_{\phi} g & \nabla_{\phi} g \frac{\nabla_{\theta} [(\tilde{y}-y)^2 + (\tilde{y}-\hat{y})^2]}{\nabla_{\phi} [(\tilde{y}-y)^2 + (\tilde{y}-\hat{y})^2]} \end{bmatrix} \\
&= \begin{bmatrix} \nabla_{\phi} g & \nabla_{\phi} g \frac{2(\hat{y}-\tilde{y})\nabla_{\theta} f}{2(\tilde{y}-y)\nabla_{\phi} g + 2(\tilde{y}-\hat{y})\nabla_{\phi} g} \end{bmatrix} \\
&= \begin{bmatrix} \nabla_{\phi} g & \frac{(\hat{y}-\tilde{y})\nabla_{\theta} f}{(\tilde{y}-y) + (\tilde{y}-\hat{y})} \end{bmatrix} \\
&\approx [\nabla_{\phi} g \quad -\nabla_{\theta} f], \quad \text{because } |\tilde{y} - y| \ll |\tilde{y} - \hat{y}|.
\end{aligned} \tag{7}$$

Reconstruction is inherently a simpler task compared to forecasting, which allows the last approximation in Eq. 7 to hold after just a few steps of initial optimization. When \tilde{y} is far distinct from original labels y , the reconstructed series \tilde{y} becomes nearly unpredictable, leading to instability in the optimization process. Therefore, adding a constraint on g can interfere with the convergence of the predictor model. To address this, Eq. 7 offers an optional assurance of gradient constraint, which uses $\|\nabla_{\theta} f\| \leq \delta$ as a surrogate for maintaining stability during optimization.

The constrained form of the optimization is equivalent to the penalized form using *Lagrangian Duality*. Eq. 3 can be rewritten as:

$$\begin{aligned}
\underset{\theta, \phi}{\text{minimize}} \quad \mathcal{L} &= \|g(y; \phi) - y\| + \|g(y; \phi) - f(x; \theta)\| \\
&\quad + \beta \|\nabla_{\theta} f(x; \theta)\|.
\end{aligned} \tag{8}$$

For readers who are familiar with Reinforcement Learning, this derivation resembles the transfer from a constrained optimization to a penalized one (e.g., from TRPO [32] to PPO [33]). In brief, while the penalized form is theoretically equivalent to the constrained form, it is challenging to choose a fixed β that works universally across all datasets or even within a single dataset (because intrinsic characteristics can vary over time). Thus, a more general form of constraint is required to better serve the penalty, similar to the concept of gradient clipping in PPO.

Note that $\nabla_{\theta} f \leq \delta$ implies the *Lipchitz condition* for an arbitrary function f . This means

$$\|f(x_1; \theta) - f(x_2; \theta)\| \leq C(\theta) \|x_1 - x_2\|, \tag{9}$$

where $C(\theta)$ is a constant with respect to the parameter θ . When considering a typical Fully Connected Layer defined as $f(x; W, b) = \sigma(Wx + b)$, the condition becomes

$$\begin{aligned}
&\|\sigma(Wx_1) - \sigma(Wx_2)\| \\
&\approx \|(\sigma(x_0) + \sigma'(x_0)(Wx_1 - x_0)) - (\sigma(x_0) + \sigma'(x_0)(Wx_2 - x_0))\|, \quad \text{by Taylor expansion} \\
&= \|\sigma'(x_0)(W(x_1 - x_2))\| \\
&\leq \sigma'_{max} \|W\| \|x_1 - x_2\| \\
&\leq C(W) \|x_1 - x_2\|.
\end{aligned} \tag{10}$$

When the derivative of activation function σ has an upper bound σ'_{max} (as is often the case for common activation functions like ReLU, Sigmoid, etc.), the Lipchitz condition holds as long as

$$\|W(x_1 - x_2)\| \leq C(W, b) \|x_1 - x_2\|. \tag{11}$$

We expect the constant C to be relatively small so that the penalty works. In fact, C here corresponds to the spectral norm of the matrix W , which is defined as

$$\|W\|_2 = \max_{x \neq 0} \frac{\|Wx\|}{\|x\|}. \tag{12}$$

By applying the Spectral Norm Regularization (SNR) in Eq. 6, we can ensure the constant C equals to exactly 1.

However, in practice, SNR have limitations when applied to the parameter matrix in self-attention mechanisms. This phenomenon is termed *entropy catastrophe* as discussed by [10]. In this paper, by analyzing the sharpness of different components in the predictor model, we propose to use pre-SNR and post-SNR combined, which specifically normalizes the first and last linear layer in the TSF models (see Section 3.4).

D Implementation Details of $g(\cdot; \phi)$

As introduced in Section 2.2, we propose a simple enough reconstruction network $g(\cdot; \phi)$ that serves our objective. Despite its simplicity, the architecture incorporates some special designs that enhance its performance. Specifically, these include the *conv-concat layer* and the *point-wise FFN*, which are detailed in Appendix D.1 and Appendix D.2, respectively.

D.1 Conv-concat Layer

Transpose and Unfold. The implementation details of the conv-concat layer involve two key operations that are designed for the following two benefits:

1. The convolution outputs can be concatenated into embeddings of the same length, enabling features from different frequencies to be ideally fused into one embedding.
2. The features are evenly arranged along the temporal dimension, ensuring that each embedding in the sequence has the same large Receptive Field.

To achieve these benefits, we introduce a two-step operation: **Transpose** and **Unfold**, which work together to ensure both uniform embedding structure and large Receptive Fields.

Specifically, we set kernel size = 3, stride = 2, padding = 1, and the number of kernels doubled for each subsequent layer. Using this setup, as illustrated in Figure 9, we ensure that the number of features remains invariant across different layers, with only the shape of the features changing. Now we can fuse the outputs from different convolution layers together by flattening/unfolding the features to the original shape of $(L \times 1)$. Again, considering the effectiveness of point-wise FFN presented in Appendix D.2, we expect the concatenated features to be near-equally arranged along the temporal dimension to preserve the sequential relationships in the embedding. To achieve this, we first transpose the features and then unfold them. This practice can ensure a Receptive Field of $(2^{l+1} - 1)$ wide for each embedding, where l is the total number of convolution layers.

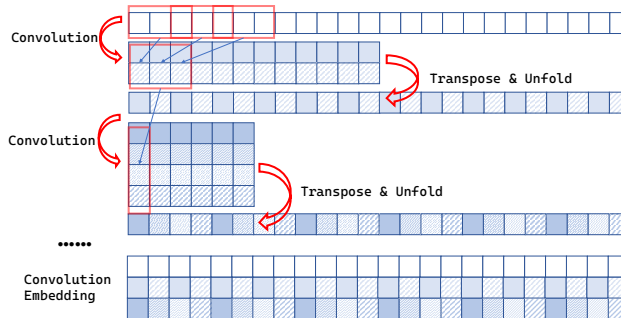


Figure 9: The illustration of transpose and unfold operation in the Convolution Encoder.

Effective Receptive Field. As what was proposed by [23], the Effective Receptive Field (ERF) is a reasonable consideration for designing convolution-based architectures. To evaluate the ERF of our conv-concat layer, we input an impulse function and visualize the resulting ERF, as shown in Figure 10. The visualization demonstrates that, without requiring an extra-large convolution kernel, our proposed method achieves a near-global ERF. This is made possible by combining the outputs from different layers, each capturing distinct frequency patterns.

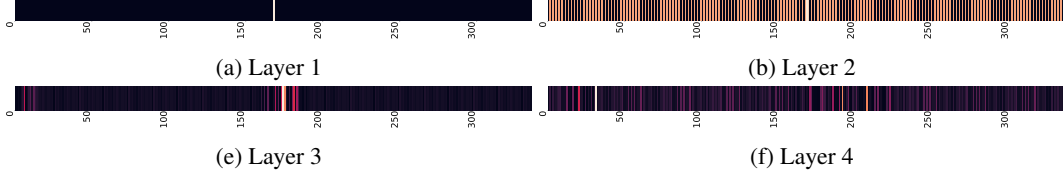


Figure 10: Effective Receptive Field (ERF) of the proposed conv-concat layer. By the transpose and unfold operation, the ERF of each convolution layer covers the entire input series with different frequencies.

D.2 Point-wise FFN

We employ a point-wise FFN as a parameter-sharing module to decode the outputs from the convolution layer. The FFN is essentially a two-layer MLP that resembles the common design of a linear projector in predictor models, as mentioned in Section E.3.

To further illustrate, we present the three different parameterizations of the linear projector commonly used in TSF models in Figure 11:

- **Patch-dependent Design:** PATCHTST [27] adopts a patch-dependent linear projector (shown in Figure 11(a)) that first flattens all features within patches and utilizes an extra-large weight matrix of shape $Ld \times d$, where L is the sequence length and d is the dimension of the latent embedding.
- **Patch-independent Design:** [14] proposes that the necessity for patch-dependent designs depends on the specific task. For instance, tasks like forecasting may require patch-dependent projectors, while tasks like contrastive learning might favor a patch-independent design (shown in Figure 11(b)).
- **Point-wise Design:** Our reconstruction process does not require exploiting the patch correlations as a necessity and can even extend this independence to point-wise scope (shown in Figure 11(c)). This approach is feasible only when each point-wise embedding is sufficiently rich in information, a property achieved through our convolution layer, which provides a near-global ERF for each point.

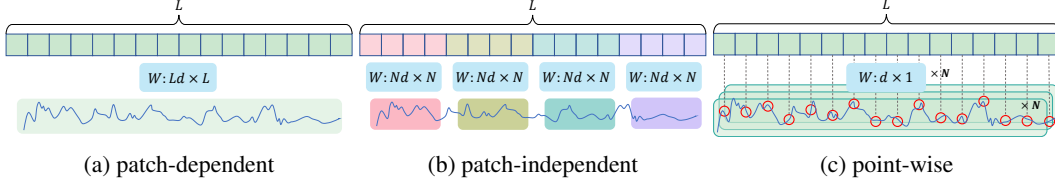


Figure 11: Three types of linear projectors.

The sharing of parameters in our linear projector allows for an increase in parallel modules. In practice, we generate multiple reconstructed samples for the same raw input sample and feed them to the predictor simultaneously. This approach inherently expands the scale of the dataset, further enhancing training efficiency.

E Further Analysis

E.1 Distribution of Reconstructed Datasets in Grid Search

The distribution of sampled predictions is shown in Figure 12. The predictions are evaluated using three loss metrics: (1) **Prediction loss:** $\ell_{pred} = \|\hat{y} - \tilde{y}\|$, (2) **Reconstruction loss:** $\ell_{rec} = \|\tilde{y} - y\|$, and (3) **Target loss:** $\ell_{target} = \|\hat{y} - y\|$. In Figure 12, scatter points illustrate the relationships among these losses across various candidate datasets generated by $g(\cdot; \phi)$ on the ETTh1 dataset. Each scatter point is colored according to the mean reconstruction loss (ℓ_{rec}) of its corresponding dataset. Lighter colors (e.g., yellow) represent datasets with higher ℓ_{rec} , while darker colors (e.g., purple) correspond to datasets with lower ℓ_{rec} .

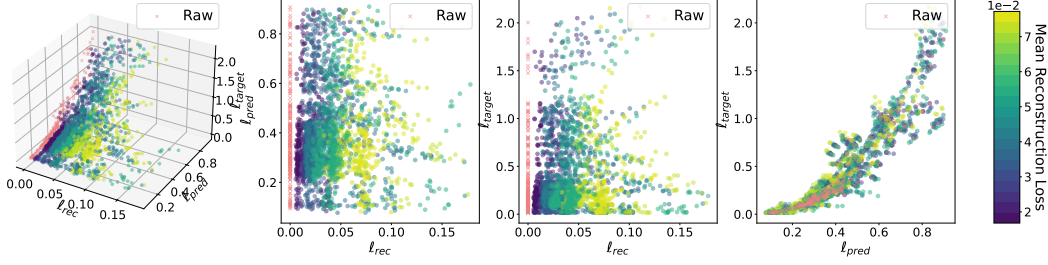


Figure 12: Distribution of losses of candidate datasets generated by $g(\cdot; \phi)$ on ETTh1.

The distribution is visualized across three projections:

1. $\ell_{rec}-\ell_{pred}$ Plane illustrates the relationship between the reconstruction loss ℓ_{rec} and the prediction loss ℓ_{pred} , both of which are actively optimized during training. As ℓ_{rec} decreases (darker colors), the points in the distribution become more condensed, indicating reduced flexibility in the candidate datasets. This trend suggests that datasets with very low reconstruction loss may lack the diversity needed for optimal predictor performance.
2. $\ell_{rec}-\ell_{target}$ Plane highlights the relationship between the reconstruction loss ℓ_{rec} and the target loss ℓ_{target} , where ℓ_{target} serves as the primary evaluation metric for predictor performance. Interestingly, datasets closer to the raw data (darker colors, with lower ℓ_{rec}) do not consistently lead to better ℓ_{target} values. This observation, which indicates that overly strict reconstruction constraints may hinder prediction quality, is further supported by Figure 3.
3. $\ell_{pred}-\ell_{target}$ Plane directly examines prediction performance, as \hat{y} is involved in calculating both ℓ_{pred} and ℓ_{target} . Notably, candidate datasets with intermediate distances from the raw data (green points) demonstrate better generalization. These datasets are characterized by relatively higher ℓ_{pred} and lower ℓ_{target} and are distributed more toward the bottom-right region of the plane, reflecting improved prediction quality.

These results suggest that datasets with moderate reconstruction loss — neither too high nor too low — strike a better balance between flexibility and generalization. This balance ultimately leads to improved predictor performance, as overly strict reconstruction constraints may limit model adaptability, while overly high reconstruction loss may fail to capture meaningful patterns.

E.2 Demystifying the Self-supervision in SCAM

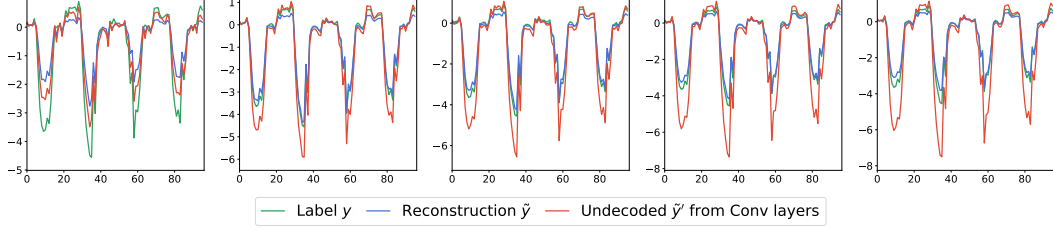
Conv-concat Layers as Feature Amplifier. In theory, the reconstruction network can be extended to larger scales as it does not interfere with inference efficiency. However, in our implementation, it is kept as simple as possible to prioritize training efficiency. Despite its simplicity, our observations reveal that the two different components of the reconstruction network function in distinct ways, which offers insights into designing more effective reconstruction networks.

As mentioned in Appendix D.2, the FFN in $g(\cdot; \phi)$ is designed point-wise, decoding the concatenated outputs of the convolution layers for each point independently. To further investigate the utility of conv-concat layers, we skip the initial linear layers and activation functions in $g(\cdot; \phi)$, directly applying the final linear transformation to the latent outputs of the conv-concat layers. This process generates an intermediate series, which we term as undecided \tilde{y}' .

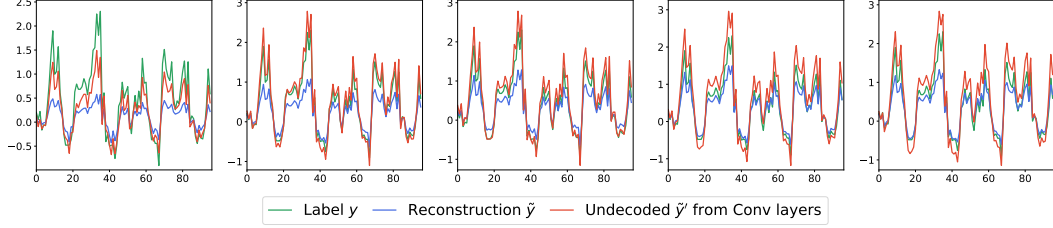
Figure 13 shows that the \tilde{y}' (red plots) effectively amplifies the sparse spiking signals present in the raw data. This behavior can be interpreted as the conv-concat layers acting as a **feature amplifier**, emphasizing and enlarging important patterns in the input data.

Channel-wise Distribution Alignment. Distribution shift, a core challenge in long-term Time Series Forecasting (TSF), is decisive for a TSF model to generalize on future data after training. The most widely adopted approach to address this issue is *Reversible Instance Normalization* (RevIn) [12, 20], which aligns the distributions of historical and future data.

While RevIn significantly improves the performance of TSF models, it falls short in aligning distributions *across channels in the multivariate forecasting setting*. Figure 14 highlights this limitation:



(a) Visualization of \tilde{y} , \tilde{y}' and y during training on Channel 1 of ETTh1. Epochs displayed here are 1, 2, 3, 4, 10.



(b) Visualization of \tilde{y} and \tilde{y}' during training and y on Channel 4 of ETTh1. Epochs displayed here are 1, 2, 3, 4, 10.

Figure 13: Visualization our difference components in $g(\cdot; \phi)$.

even when the raw data y is normalized by RevIn, the distribution distances (measured by the KL divergence metric) remain significant, as shown in the leftmost plots of all subfigures.

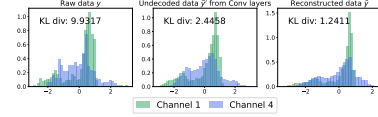
In this view, the proposed reconstruction network $g(\cdot; \theta)$ effectively serves as a general **channel-wise distribution alignment** mechanism. Interestingly, when examining the intermediate undecided \tilde{y}' across channels, we observe that, although the sparse features are amplified, the distribution distances are reduced compared to those in the raw data. Overall, the final reconstructed series exhibits better alignment across channels. However, exceptions such as Channels 3 and 6 (see Figure 14(c)) demonstrate that the alignment is not uniform across all channels.

For models designed with *channel-independence* (CI), such as PATCHTST [27] and CYCLENET [17], aligning distributions across channels is of critical importance, especially when trained on datasets with a large number of variates. The channel-wise alignment introduced by our self-supervised reconstruction task provides an effective solution to distribution shifts, thereby enhancing the performance of CI predictor models.

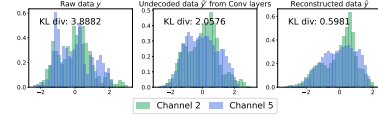
Evolution of Adaptive Mask in SCAM. In Section 4.3, we have explored the benefits of the adaptive mask in SCAM from a Multiple Instance Learning (MIL) view, highlighting its sensitivity to instances with varying deviations and its ability to apply different masking strategies accordingly.

In this part, we further visualize the evolution process of the adaptive mask during training on real datasets, using ETTh1 as an example, as shown in Figure 15.

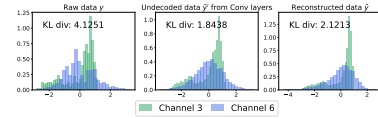
At the very first epoch, the model heavily relies on the prediction \hat{y} to reconstruct the series \tilde{y} . This benefits the convergence of both the predictor model $f(\cdot; \theta)$ and the reconstruction network $g(\cdot; \phi)$. As previously analyzed, the reconstructed series \tilde{y} aligns the data distribution, enabling $f(\cdot; \theta)$ to learn effectively from \tilde{y} . Correspondingly, the prediction \hat{y} in the first epoch is basically a draft with smooth curvature, preventing \tilde{y} from quickly overfitting the noisy raw labels y . In subsequent epochs, the proportion of gray masks applied to the loss term $\|\hat{y}, y\|$



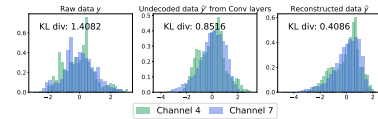
(a) Distributions of Channels 1 and 4.



(b) Distributions of Channels 2 and 5.



(c) Distributions of Channels 3 and 6.



(d) Distributions of Channels 4 and 7.

Figure 14: Distribution alignment for channels in ETTh1 with data all normalized by RevIN.

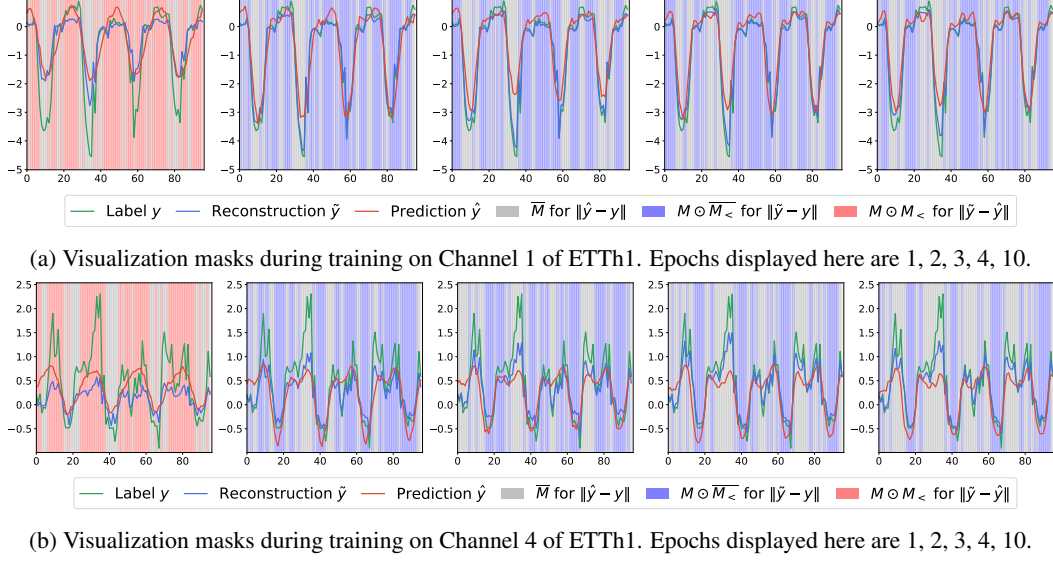


Figure 15: Evolution of the adaptive masks in SCAM during training.

increases. This indicates that the model progressively emphasizes a more precise fitting to the true labels, resulting in improved reconstruction and prediction quality.

In comparison with the case study in Section 4.3, the adaptive mask tends to collapse more rapidly from intermediate states where all three masking strategies are simultaneously active. This is possibly due to the noisy and unpredictable nature of real-world datasets. We plan to explore less aggressive strategies compared to binary masking, which hopefully will increase the robustness of the current method.

E.3 In-depth Examination on SNR

We further verify the effectiveness of SNR by analyzing the loss landscape. Transformer-based models, as discussed, are more prone to overfitting, particularly on noisy datasets. This weakens our adaptive mask’s ability to discard overfitted components, as ℓ_{pred} — the predictor’s training loss — also contributes to overfitting. Gradient penalty offers a solution to this issue. For TSF models specifically, where both inputs and outputs are time series with abrupt distribution shifts, parameter robustness is critical for mitigating overfitting. Previous works [46, 26] have shown that regulating parameters via their spectral norm enhances stability against input perturbations, which is particularly beneficial in TSF.

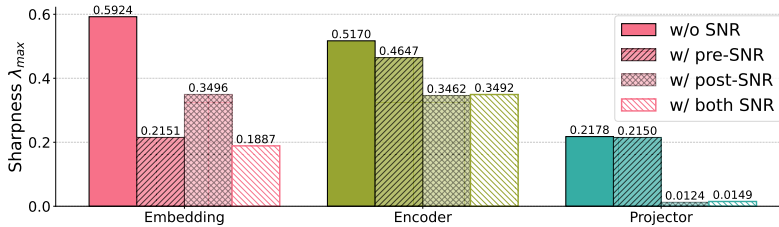


Figure 16: Sharpness of difference components in iTRANS.

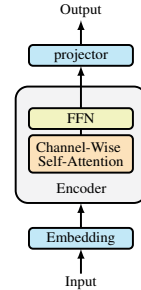


Figure 17: iTRANS as a TST example

In Figure 16, the bars represent the sharpness of different components in iTRANS, divided into three parts: embedding, encoder, and projector (see Figure 17). The embedding and projector are linear layers, while the encoder comprises channel-wise attention blocks. This architectural pattern is

common among Time Series Transformers (TSTs), with the encoder being the primary focus and less emphasis placed on pre- or post-encoder linear layers.

Without SNR, the input linear layer (embedding) exhibits the highest sharpness, indicating it is the most overfitted component (see red bars). This suggests that overfitting in Transformers originates not only from self-attention mechanisms but also from the linear layers. By applying SNR to the pre- and post-encoder linear layers (Section 3.4), we observe smoother loss landscapes, validating SNR’s ability to reduce sharpness effectively.

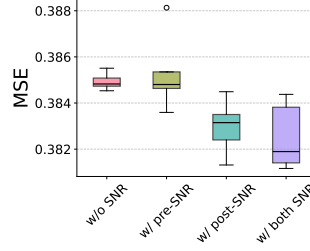


Figure 18: Empirical results on variants of SNR.

To determine the best practices for SNR, we conduct multiple runs with different random seeds to evaluate various design choices. As shown in Figure 18, applying SNR to the post-encoder linear layer or both linear layers proves most effective: ‘post-SNR’ achieves lower mean metrics and reduced variance, while ‘both SNR’ yields better mean performance but with higher variance. We recommend both practices, depending on the use case, and adopt ‘both SNR’ for all tests in this paper.

F Related Work Revisit

In this part, we will introduce some popularly adopted methods for TSF, in which our baseline models are included.

Channel-independent Transformers. Time Series Transformers (TST) [53, 40, 54] have recently led to significant progress in the TSF problem, demonstrating convincing superiority over traditional methods and convolution-based models. Inspired by [48], [27] incorporates the *Channel Independent* (CI) design (sharing weights across all channels) to introduce PATCHTST, a new state-of-the-art (SOTA) model that significantly benefits from CI and the patching operation. Multiple works follow this practice and achieve excellent performance in TSF [6, 19, 50].

Channel-wise Transformers. Building on TST, more recent research has focused on designing Transformers capable of capturing channel dependencies inherent in multivariate time series data. Notable examples include CROSSFORMER [51], iTRANSFORMER (iTRANS) [21], DSFORMER [47], and CARD [37]. These models shed light on exploiting inter-series relationships to improve forecasting accuracy. Furthermore, having observed that Time Series Transformers are inherently unstable due to a sharp loss scape, [10] propose a sharpness-aware optimizer to mitigate such issues. Their work focuses on an optimization-level approach involving a two-step backward. Nonetheless, channel-wise Transformers still suffer from overfitting on small datasets. By sharpness analysis, our proposed SCAM locates the overfitting issue and provides a solution from a data-level perspective.

Linear or MLP-based Models. In contrast to the quadratic complexity of Transformers, lightweight linear or MLP-based models have emerged as competitive alternatives offering simplicity and efficiency. RLINEAR and RMLP [15] verify that a vanilla linear model or a 2-layer MLP, when combined with a widely-adopted normalization method [12], can achieve near SOTA performance in TSF. Further research [52] on channel dependencies within linear and MLP-based models has yielded performance improvements over previous CI approaches. Moreover, the models [44, 45] that directly learn linear regression or MLP-based models on complex frequency features have achieved remarkable performances. Most recently, SPARSETSF [16], a highly lightweight model, incorporates 1D convolutions as down-sampling modules and learns linear parameters on the down-sampled values of the original series. CYCLENET [17], a SOTA model that explicitly captures periodic trend features to enhance vanilla linear or MLP-based models to be on par with Transformer-based models.

G Experiment Details

G.1 Datasets

We conduct experiments on 11 real-world datasets to evaluate the performance of the proposed SCAM. The datasets are detailed below.

- **ETT** [53]: This dataset contains 7 factors of electricity transformers, recorded between July 2016 and July 2018. The subsets ETTh1 and ETTh2 are recorded hourly, while ETTm1 and ETTm2 are recorded every 15 minutes.
- **Electricity** [40]: This dataset records the hourly electricity consumption of 321 clients.
- **Traffic** [40]: This dataset collects hourly road occupancy rates measured by 862 sensors across the San Francisco Bay Area freeways, spanning from January 2015 to December 2016.
- **Weather** [40]: This dataset includes 21 meteorological factors, recorded every 10 minutes at the Weather Station of the Max Planck Biogeochemistry Institute in 2020.
- **PeMS**: This dataset contains public traffic network data from California, collected at 5-minute intervals. We use the same four subsets (PeMS03, PeMS04, PeMS07, PeMS08) as adopted in iTRANSFORMER (iTRANS) [21].

For the ETT datasets, we divide them by ratio $\{0.6, 0.2, 0.2\}$ into train set, validation set, and test set. For Electricity, Traffic, and Weather, we follow the same split ratio of $\{0.7, 0.1, 0.2\}$ as in TIMESNET [41, 53, 40]. For the PeMS datasets, we split them using the ratio $\{0.6, 0.2, 0.2\}$ following the same setting as iTRANS [21]. All datasets are scaled using the mean and variance of their respective training sets, a standard practice in TSF [41]. The statistics of all used datasets are listed in Table 4.

Table 4: Statistics of evaluation datasets.

Datasets	ETTh1	ETTh2	ETTm1	ETTm2	Electricity	Traffic	Weather	PeMS03	PeMS04	PeMS07	PeMS08
# of TS Variates	7	7	7	7	321	862	21	358	307	883	170
TS Length	17420	17420	69680	69680	26304	17544	52696	26209	16992	28224	17856

G.2 Backbones

We evaluate the proposed SCAM against the following baseline backbone models:

1. MLP [15], a 2-layer MLP model combined with Reversible Instance Normalization [12].
2. CYCLENET [17], a 2-layer MLP equipped with efficient cycle modeling that belongs to a general seasonal-trend decomposition method (Cycle/MLP in the original paper).
3. iTRANS [21], a Transformer-based model that computes attention scores on the inverted series along the channel dimension.
4. PATCHTST [27], a Channel-Independent Transformer-based model that uses patching to tokenize the input.

It should be pointed out that the scale of a time series dataset is determined by a combination of the number of variates and the length of the dataset. Therefore, a fair comparison should take both factors into account. In our experiments, we observe that some baseline models, such as iTRANS, benefit greatly from datasets with a larger number of variates, while others, like PATCHTST, tend to perform better on longer datasets.

G.3 Reproducibility

Hyperparameters and Settings. All experiments and methods are implemented in Python and PyTorch [29] and conducted on two Nvidia RTX A5000 Ada generation GPUs (32GB VRAMs) and two Nvidia RTX A6000 GPUs (48GB VRAMs). We use the ADAM optimizer [13] with a learning rate initialized as $\eta = 0.001$ for all settings. Unlike prior works [21, 16] that set a fixed, small number of training epochs, we adopt an early stopping strategy based on the MSE metric of the validation set, with a patience of 20 epochs.

For the reconstruction network $g(\cdot; \phi)$, the hyperparameters are detailed in Table 5.

We use 4 convolution layers in total, with consistent settings for kernel size, stride, and padding size as explained in Appendix D.1. Dim_multiplier represents the expansion ratio of convolution channels. The channels for the four convolution layers are set to 1, 2, 4, and 8, respectively, and are further multiplied by 4 to increase the model’s capacity. Hidden_dim is the dimension size in the FFN, and # of series indicates that we use 8 point-wise linear projectors in parallel as explained in Appendix D.2

Table 5: Hyperparameters of the reconstruction network $g(\cdot; \phi)$.

# of convolution layers	4
dim_multiplier	4
hidden_dim	128
# of series	8

and Figure 11. The hyperparameter settings provided in Table 5 are applied consistently across all datasets.

Rerun Baselines as Additional Comparisons. To ensure fair comparisons with baseline results, we include both the results reported in the original papers and the results from our own re-implementations. Specifically: The MLP and CYCLENET results are taken from CYCLENET paper [17]. The PATCHTST and ITRANS results are from the ITRANS paper [21], as the PATCHTST paper [27] does not provide results with a look-back length of 96.

While the results from the original papers and our reruns show no major discrepancies, minor differences do exist. To provide complete transparency, we present both in Table 8 and Table 9 in Appendix H. Results from the original papers are more reliable as they reflect the authors’ intended implementations, while our reruns ensure consistency in training settings for direct comparison.

The Result Discrepancy on PeMS Datasets. We also evaluate the larger traffic dataset, PeMS, which has been previously examined in both ITRANS and CYCLENET. However, we observe major discrepancies between our results and those reported in the original papers [21, 17].

While the original papers state that prediction lengths of $\{12, 24, 48, 96\}$ were used, their reported results closely align with what we obtain using prediction lengths of $\{12, 24, 36, 48\}$. The issue of reproduction inconsistencies is also widely discussed in the ITRANSFORMER GitHub issues. For reference, we provide the results obtained using our settings, which we hope will aid in clarifying these discrepancies.

G.4 Efficiency

Table 6: The efficiency analysis of SCAM. All metrics are measured on the Electricity dataset with a batch size of 32.

	# of parameters	Max Memory Allocated (GB)	Training Time (ms/iter)
MLP	24.8K	0.102	6.126
+SCAM	52.4K	1.095	30.451
CYCLENET	78.7K	0.099	6.879
+SCAM	106K	1.092	30.832
PATCHTST	338K	1.281	28.074
+SCAM	365K	2.072	53.044
ITRANS	3.3M	0.791	20.395
+SCAM	3.3M	1.729	44.357

The SCAM method introduces an additional lightweight reconstruction network to aid the training. The additional computation cost is only introduced in training, because the additional module is discarded like a *scaffold*.

For the training efficiency, the baselines we adopted are acknowledged for their low cost. We only introduce a *constant* increase in memory and time consumption, enabling our method to be integrated into backbones that scale in parameters.

H More Experiment Results

In this section, we present detailed results from the previously mentioned experiments:

- **Tables 8 and 9:**
 - Summarize the main experiments on the ETT, Electricity, Traffic, and Weather datasets, with detailed breakdowns of different prediction lengths provided.
 - Baseline results in **Table 8** are taken from the original papers.
 - Baseline results in **Table 9** are reproduced by us.
- **Table 7:**
 - Reports experiments on the PeMS datasets, including baseline results from our runs.
- **Tables 10 and 11:**
 - Provide the complete results of the ablation studies.

In Table 7, 8 and 9, color **RED** indicates better performance and color **BLUE** indicates worse performance.

Table 7: Full results of experiments on PeMS datasets, comparing backbone models and their integration with our proposal. All baseline results are reproduced by us.

Models		MLP		+Ours		CYCLENET		+Ours		PATCHTST		+Ours		ITRANS		+Ours	
	Metric	MSE	MAE	MSE	MAE	MSE	MAE	MSE	MAE	MSE	MAE	MSE	MAE	MSE	MAE	MSE	MAE
PeMS03	12	0.083	0.191	0.082	0.189	0.073	0.179	0.072	0.178	0.078	0.186	0.072	0.176	0.075	0.186	0.074	0.180
	24	0.138	0.246	0.132	0.240	0.108	0.218	0.106	0.216	0.123	0.234	0.104	0.212	0.097	0.207	0.089	0.198
	36	0.196	0.297	0.189	0.291	0.147	0.256	0.144	0.255	0.172	0.276	0.136	0.244	0.127	0.237	0.130	0.242
	48	0.257	0.344	0.198	0.304	0.182	0.288	0.178	0.291	0.221	0.317	0.160	0.264	0.166	0.273	0.174	0.285
	Avg.	0.168	0.269	0.150	0.256	0.127	0.235	0.125	0.235	0.148	0.253	0.118	0.224	0.116	0.226	0.117	0.226
PeMS04	12	0.103	0.211	0.103	0.211	0.092	0.198	0.091	0.197	0.101	0.208	0.084	0.190	0.084	0.188	0.080	0.183
	24	0.168	0.273	0.167	0.273	0.137	0.244	0.137	0.244	0.162	0.268	0.116	0.228	0.121	0.228	0.108	0.213
	36	0.246	0.335	0.243	0.333	0.187	0.289	0.187	0.289	0.227	0.321	0.147	0.261	0.151	0.257	0.139	0.244
	48	0.326	0.390	0.320	0.387	0.235	0.329	0.234	0.328	0.297	0.367	0.168	0.279	0.186	0.288	0.191	0.295
	Avg.	0.211	0.302	0.208	0.301	0.163	0.265	0.162	0.265	0.197	0.291	0.129	0.240	0.135	0.240	0.130	0.234
PeMS07	12	0.079	0.185	0.080	0.185	0.069	0.171	0.069	0.171	0.076	0.180	0.068	0.169	0.063	0.159	0.060	0.154
	24	0.140	0.248	0.139	0.246	0.110	0.218	0.109	0.217	0.130	0.241	0.106	0.212	0.090	0.192	0.085	0.184
	36	0.210	0.306	0.209	0.304	0.153	0.260	0.152	0.260	0.184	0.286	0.144	0.248	0.135	0.242	0.132	0.237
	48	0.285	0.360	0.282	0.357	0.195	0.299	0.194	0.298	0.244	0.332	0.179	0.281	0.171	0.277	0.183	0.293
	Avg.	0.179	0.275	0.177	0.273	0.132	0.237	0.131	0.236	0.159	0.260	0.124	0.228	0.115	0.218	0.115	0.217
PeMS08	12	0.093	0.198	0.094	0.199	0.082	0.184	0.082	0.184	0.087	0.191	0.130	0.187	0.077	0.176	0.071	0.167
	24	0.153	0.257	0.152	0.255	0.124	0.228	0.125	0.228	0.137	0.240	0.163	0.222	0.107	0.207	0.100	0.198
	36	0.223	0.312	0.220	0.310	0.170	0.268	0.170	0.267	0.194	0.291	0.163	0.222	0.142	0.239	0.130	0.223
	48	0.297	0.362	0.293	0.360	0.220	0.307	0.218	0.305	0.255	0.334	0.223	0.276	0.204	0.293	0.200	0.293
	Avg.	0.192	0.282	0.190	0.281	0.149	0.247	0.149	0.246	0.168	0.264	0.170	0.227	0.133	0.228	0.125	0.220
Imp%	Avg.	-	-	3.24%	1.48%	-	-	0.57%	0.23%	-	-	19.61%	14.06%	-	-	2.51%	1.55%

Table 8: Full results for performance comparisons between backbone models and their integration with our proposals on ETT, Electricity, Traffic, and Weather datasets. The results for MLP and CYCLENET are taken from the CYCLENET paper [27], while the results for PATCHTST and ITRANS are from the ITRANSFORMER paper [21].

Models	MLP			+Ours		CYCLENET		+Ours		PATCHTST		+Ours		ITRANS		+Ours	
	Metric	MSE	MAE	MSE	MAE	MSE	MAE	MSE	MAE	MSE	MAE	MSE	MAE	MSE	MAE	MSE	MAE
ETTm1	96	0.383	0.401	0.373	0.396	0.375	0.395	0.368	0.390	0.414	0.419	0.373	0.398	0.386	0.405	0.373	0.401
	192	0.437	0.432	0.435	0.434	0.436	0.428	0.424	0.424	0.460	0.445	0.424	0.427	0.441	0.436	0.432	0.436
	336	0.494	0.461	0.474	0.442	0.496	0.455	0.470	0.440	0.501	0.466	0.465	0.447	0.487	0.458	0.466	0.455
	720	0.540	0.499	0.464	0.459	0.520	0.484	0.462	0.461	0.500	0.488	0.444	0.458	0.503	0.491	0.455	0.466
	Avg.	0.464	0.448	0.437	0.433	0.457	0.441	0.431	0.429	0.469	0.455	0.427	0.433	0.454	0.448	0.431	0.440
ETTm2	96	0.299	0.345	0.283	0.336	0.298	0.344	0.280	0.333	0.302	0.348	0.285	0.336	0.297	0.349	0.293	0.342
	192	0.371	0.394	0.362	0.385	0.372	0.396	0.357	0.384	0.388	0.400	0.367	0.389	0.380	0.400	0.373	0.393
	336	0.420	0.429	0.404	0.420	0.431	0.439	0.400	0.420	0.426	0.433	0.409	0.425	0.428	0.432	0.417	0.429
	720	0.438	0.450	0.413	0.435	0.450	0.458	0.409	0.436	0.431	0.446	0.419	0.442	0.427	0.445	0.424	0.442
	Avg.	0.382	0.405	0.366	0.394	0.388	0.409	0.362	0.393	0.387	0.407	0.370	0.398	0.383	0.407	0.377	0.402
ETTm1	96	0.327	0.366	0.325	0.361	0.319	0.360	0.306	0.349	0.329	0.367	0.316	0.354	0.334	0.368	0.315	0.353
	192	0.370	0.386	0.367	0.383	0.360	0.381	0.349	0.375	0.367	0.385	0.360	0.382	0.377	0.391	0.369	0.387
	336	0.404	0.410	0.400	0.405	0.389	0.403	0.379	0.394	0.399	0.410	0.393	0.402	0.426	0.420	0.403	0.412
	720	0.462	0.445	0.462	0.443	0.447	0.441	0.438	0.435	0.454	0.439	0.454	0.437	0.491	0.459	0.460	0.445
	Avg.	0.391	0.402	0.388	0.398	0.379	0.396	0.368	0.388	0.387	0.400	0.381	0.394	0.407	0.410	0.387	0.399
ETTm2	96	0.178	0.259	0.175	0.259	0.163	0.246	0.161	0.244	0.175	0.259	0.176	0.261	0.180	0.264	0.179	0.264
	192	0.242	0.302	0.240	0.300	0.229	0.290	0.225	0.286	0.241	0.302	0.241	0.300	0.250	0.309	0.241	0.302
	336	0.299	0.340	0.295	0.336	0.284	0.437	0.282	0.323	0.305	0.343	0.303	0.340	0.311	0.348	0.305	0.343
	720	0.400	0.398	0.394	0.394	0.389	0.391	0.380	0.384	0.402	0.400	0.404	0.403	0.412	0.407	0.406	0.400
	Avg.	0.280	0.325	0.276	0.322	0.266	0.341	0.262	0.309	0.281	0.326	0.281	0.326	0.288	0.332	0.283	0.327
Electricity	96	0.182	0.265	0.181	0.264	0.136	0.229	0.134	0.228	0.181	0.270	0.163	0.248	0.148	0.240	0.145	0.237
	192	0.187	0.270	0.186	0.268	0.152	0.244	0.152	0.244	0.188	0.274	0.172	0.257	0.162	0.253	0.158	0.252
	336	0.203	0.287	0.202	0.285	0.170	0.264	0.170	0.263	0.204	0.293	0.191	0.278	0.178	0.269	0.176	0.271
	720	0.244	0.319	0.243	0.317	0.212	0.299	0.210	0.296	0.246	0.324	0.239	0.319	0.225	0.317	0.212	0.306
	Avg.	0.204	0.285	0.203	0.283	0.168	0.259	0.166	0.258	0.205	0.290	0.191	0.275	0.178	0.270	0.173	0.267
Traffic	96	0.510	0.331	0.477	0.301	0.458	0.296	0.420	0.275	0.462	0.295	0.433	0.280	0.395	0.268	0.374	0.247
	192	0.505	0.327	0.478	0.300	0.457	0.295	0.437	0.283	0.466	0.296	0.447	0.287	0.417	0.276	0.399	0.259
	336	0.518	0.332	0.492	0.305	0.470	0.299	0.453	0.291	0.482	0.304	0.455	0.285	0.433	0.283	0.419	0.269
	720	0.553	0.350	0.531	0.328	0.502	0.314	0.482	0.310	0.514	0.322	0.486	0.302	0.467	0.302	0.451	0.291
	Avg.	0.522	0.335	0.494	0.308	0.472	0.301	0.448	0.290	0.481	0.304	0.455	0.288	0.428	0.282	0.411	0.266
Weather	96	0.181	0.219	0.176	0.214	0.158	0.203	0.158	0.203	0.177	0.218	0.169	0.211	0.174	0.214	0.173	0.213
	192	0.228	0.259	0.223	0.256	0.207	0.247	0.206	0.244	0.225	0.259	0.215	0.251	0.221	0.254	0.223	0.257
	336	0.282	0.299	0.279	0.295	0.262	0.289	0.260	0.285	0.278	0.297	0.274	0.293	0.278	0.296	0.278	0.296
	720	0.357	0.347	0.355	0.345	0.344	0.344	0.343	0.342	0.354	0.348	0.353	0.345	0.358	0.347	0.353	0.344
	Avg.	0.262	0.281	0.258	0.278	0.243	0.271	0.242	0.268	0.259	0.281	0.253	0.275	0.258	0.278	0.257	0.278
Imp%	Avg.	-	-	3.24%	2.60%	-	-	3.92%	3.40%	-	-	4.48%	2.97%	-	-	3.24%	1.94%

Table 9: Full results for performance comparisons between backbone models and them integrated with our proposals on ETT, electricity, traffic and weather datasets. All baseline results are run ourselves

Models	MLP		+Ours		CYCLENET		+Ours		PATCHTST		+Ours		ITRANS		+Ours		
	Metric	MSE	MAE	MSE	MAE	MSE	MAE	MSE	MAE	MSE	MAE	MSE	MAE	MSE	MAE	MSE	MAE
ETTh1	96	0.380	0.399	0.373	0.396	0.379	0.400	0.368	0.390	0.390	0.407	0.373	0.398	0.383	0.405	0.373	0.401
	192	0.444	0.428	0.435	0.434	0.437	0.432	0.424	0.424	0.461	0.446	0.424	0.427	0.434	0.433	0.432	0.436
	336	0.478	0.444	0.474	0.442	0.477	0.446	0.470	0.440	0.486	0.457	0.465	0.447	0.470	0.452	0.466	0.455
	720	0.478	0.475	0.464	0.459	0.469	0.466	0.462	0.461	0.484	0.469	0.444	0.458	0.464	0.470	0.455	0.466
	Avg.	0.445	0.437	0.437	0.433	0.441	0.436	0.431	0.429	0.455	0.445	0.427	0.433	0.438	0.440	0.431	0.440
ETTh2	96	0.293	0.343	0.283	0.336	0.297	0.347	0.280	0.333	0.298	0.345	0.285	0.336	0.321	0.362	0.293	0.342
	192	0.368	0.391	0.362	0.385	0.374	0.396	0.357	0.384	0.394	0.401	0.367	0.389	0.394	0.408	0.373	0.393
	336	0.419	0.427	0.404	0.420	0.417	0.432	0.400	0.420	0.418	0.429	0.409	0.425	0.449	0.447	0.417	0.429
	720	0.427	0.443	0.413	0.435	0.430	0.447	0.409	0.436	0.437	0.454	0.419	0.442	0.435	0.449	0.424	0.442
	Avg.	0.377	0.401	0.366	0.394	0.380	0.406	0.362	0.393	0.387	0.407	0.370	0.398	0.400	0.417	0.377	0.402
ETTm1	96	0.348	0.371	0.325	0.361	0.315	0.358	0.306	0.349	0.339	0.370	0.316	0.354	0.351	0.378	0.315	0.353
	192	0.388	0.391	0.367	0.383	0.359	0.382	0.349	0.375	0.381	0.393	0.360	0.382	0.393	0.399	0.369	0.387
	336	0.422	0.412	0.400	0.405	0.389	0.407	0.379	0.394	0.411	0.413	0.393	0.402	0.422	0.421	0.403	0.412
	720	0.493	0.451	0.462	0.443	0.454	0.441	0.438	0.435	0.474	0.449	0.454	0.437	0.487	0.460	0.460	0.445
	Avg.	0.413	0.406	0.388	0.398	0.379	0.397	0.368	0.388	0.401	0.406	0.381	0.394	0.413	0.414	0.387	0.399
ETTm2	96	0.186	0.270	0.175	0.259	0.164	0.248	0.161	0.244	0.180	0.263	0.176	0.261	0.189	0.275	0.179	0.264
	192	0.249	0.309	0.240	0.300	0.228	0.289	0.225	0.286	0.248	0.310	0.241	0.300	0.260	0.318	0.241	0.302
	336	0.308	0.345	0.295	0.336	0.285	0.328	0.282	0.323	0.307	0.345	0.303	0.340	0.326	0.359	0.305	0.343
	720	0.404	0.398	0.394	0.394	0.387	0.387	0.380	0.384	0.411	0.404	0.404	0.403	0.423	0.412	0.406	0.400
	Avg.	0.287	0.331	0.276	0.322	0.266	0.313	0.262	0.309	0.287	0.331	0.281	0.326	0.299	0.341	0.283	0.327
Electricity	96	0.187	0.267	0.181	0.264	0.136	0.230	0.134	0.228	0.181	0.268	0.163	0.248	0.161	0.251	0.145	0.237
	192	0.191	0.272	0.186	0.268	0.154	0.246	0.152	0.244	0.193	0.277	0.172	0.257	0.178	0.267	0.158	0.252
	336	0.206	0.288	0.202	0.285	0.171	0.264	0.170	0.263	0.199	0.286	0.191	0.278	0.193	0.281	0.176	0.271
	720	0.251	0.325	0.243	0.317	0.212	0.299	0.210	0.296	0.240	0.319	0.239	0.319	0.213	0.306	0.212	0.306
	Avg.	0.209	0.288	0.203	0.283	0.168	0.260	0.166	0.258	0.203	0.287	0.191	0.275	0.186	0.276	0.173	0.267
Traffic	96	0.504	0.314	0.477	0.301	0.432	0.292	0.420	0.275	0.468	0.301	0.433	0.280	0.403	0.276	0.374	0.247
	192	0.522	0.330	0.478	0.300	0.443	0.294	0.437	0.283	0.474	0.305	0.447	0.287	0.423	0.283	0.399	0.259
	336	0.534	0.334	0.492	0.305	0.460	0.304	0.453	0.291	0.498	0.324	0.455	0.285	0.441	0.292	0.419	0.269
	720	0.540	0.337	0.531	0.328	0.489	0.321	0.482	0.310	0.547	0.340	0.486	0.302	0.465	0.303	0.451	0.291
	Avg.	0.525	0.329	0.494	0.308	0.456	0.303	0.448	0.290	0.497	0.317	0.455	0.288	0.433	0.288	0.411	0.266
Weather	96	0.192	0.232	0.176	0.214	0.165	0.209	0.158	0.203	0.185	0.225	0.169	0.211	0.211	0.257	0.173	0.213
	192	0.237	0.266	0.223	0.256	0.209	0.248	0.206	0.244	0.229	0.262	0.215	0.251	0.255	0.285	0.223	0.257
	336	0.290	0.304	0.279	0.295	0.269	0.292	0.260	0.285	0.283	0.302	0.274	0.293	0.303	0.319	0.278	0.296
	720	0.366	0.352	0.355	0.345	0.348	0.344	0.343	0.342	0.361	0.351	0.353	0.345	0.370	0.362	0.353	0.344
	Avg.	0.271	0.288	0.258	0.278	0.248	0.273	0.242	0.268	0.264	0.285	0.253	0.275	0.285	0.306	0.257	0.278
Imp%	Avg.	-	-	4.11%	2.56%	-	-	2.52%	2.18%	-	-	5.48%	3.61%	-	-	5.51%	4.17%

Table 10: Full results of ablation study with backbone predictor as CYCLENET.

Models	CYCLENET		+SNR		+SCAM		+both		
Metric	MSE	MAE	MSE	MAE	MSE	MAE	MSE	MAE	
ETTh1	96	0.381	0.399	0.374	0.392	0.372	0.393	0.368	0.390
	192	0.438	0.426	0.432	0.423	0.424	0.424	0.424	0.424
	336	0.478	0.446	0.475	0.444	0.470	0.440	0.470	0.440
	720	0.478	0.472	0.470	0.469	0.480	0.473	0.462	0.461
	Avg.	0.444	0.436	0.438	0.432	0.436	0.432	0.431	0.429
ETTh2	96	0.297	0.347	0.288	0.339	0.283	0.336	0.280	0.333
	192	0.379	0.399	0.371	0.392	0.357	0.384	0.357	0.384
	336	0.419	0.433	0.412	0.425	0.400	0.420	0.400	0.420
	720	0.430	0.447	0.415	0.437	0.421	0.440	0.409	0.436
	Avg.	0.381	0.407	0.372	0.398	0.365	0.395	0.362	0.393
ETTm1	96	0.315	0.358	0.312	0.353	0.308	0.349	0.306	0.349
	192	0.359	0.382	0.356	0.379	0.352	0.372	0.349	0.375
	336	0.389	0.407	0.384	0.400	0.385	0.402	0.379	0.394
	720	0.454	0.441	0.449	0.435	0.441	0.436	0.438	0.435
	Avg.	0.379	0.397	0.375	0.392	0.371	0.390	0.368	0.388
ETTm2	96	0.164	0.248	0.162	0.245	0.161	0.244	0.161	0.244
	192	0.228	0.289	0.227	0.287	0.226	0.287	0.225	0.286
	336	0.285	0.328	0.285	0.326	0.283	0.326	0.282	0.323
	720	0.387	0.387	0.385	0.385	0.381	0.386	0.380	0.384
	Avg.	0.266	0.313	0.265	0.311	0.263	0.311	0.262	0.309
Weather	96	0.165	0.209	0.159	0.203	0.159	0.202	0.158	0.203
	192	0.209	0.248	0.210	0.249	0.206	0.244	0.206	0.244
	336	0.269	0.292	0.267	0.291	0.260	0.285	0.260	0.285
	720	0.348	0.344	0.347	0.343	0.343	0.338	0.343	0.342
	Avg.	0.248	0.273	0.246	0.272	0.242	0.267	0.242	0.268

Table 11: Full results of ablation study with backbone predictor as ITRANS.

Models		ITRANS		+SNR		+SCAM		+both	
Metric		MSE	MAE	MSE	MAE	MSE	MAE	MSE	MAE
ETTh1	96	0.383	0.405	0.388	0.407	0.376	0.397	0.373	0.401
	192	0.434	0.433	0.446	0.441	0.434	0.436	0.432	0.436
	336	0.470	0.452	0.472	0.457	0.470	0.451	0.466	0.455
	720	0.464	0.470	0.467	0.475	0.464	0.467	0.455	0.466
	Avg.	0.438	0.440	0.443	0.445	0.436	0.438	0.431	0.440
ETTh2	96	0.321	0.362	0.331	0.370	0.296	0.344	0.293	0.342
	192	0.394	0.408	0.398	0.410	0.385	0.399	0.373	0.393
	336	0.449	0.447	0.431	0.437	0.418	0.429	0.417	0.429
	720	0.435	0.449	0.437	0.453	0.426	0.443	0.424	0.442
	Avg.	0.400	0.417	0.399	0.417	0.381	0.404	0.377	0.402
ETTm1	96	0.351	0.378	0.345	0.376	0.324	0.366	0.315	0.353
	192	0.393	0.399	0.385	0.395	0.376	0.393	0.369	0.387
	336	0.422	0.421	0.429	0.427	0.404	0.412	0.403	0.412
	720	0.487	0.460	0.494	0.461	0.461	0.447	0.460	0.445
	Avg.	0.413	0.414	0.413	0.415	0.391	0.404	0.387	0.399
ETTm2	96	0.189	0.275	0.204	0.289	0.184	0.279	0.179	0.264
	192	0.260	0.318	0.275	0.331	0.252	0.321	0.241	0.302
	336	0.326	0.359	0.324	0.358	0.323	0.357	0.305	0.343
	720	0.423	0.412	0.421	0.410	0.412	0.411	0.406	0.400
	Avg.	0.299	0.341	0.306	0.347	0.293	0.342	0.283	0.327
Weather	96	0.211	0.257	0.212	0.247	0.190	0.226	0.173	0.213
	192	0.255	0.285	0.252	0.283	0.243	0.270	0.223	0.257
	336	0.303	0.319	0.301	0.319	0.295	0.307	0.278	0.296
	720	0.370	0.362	0.367	0.357	0.366	0.353	0.353	0.344
	Avg.	0.285	0.306	0.283	0.302	0.274	0.289	0.257	0.278

NeurIPS Paper Checklist

The checklist is designed to encourage best practices for responsible machine learning research, addressing issues of reproducibility, transparency, research ethics, and societal impact. Do not remove the checklist: **The papers not including the checklist will be desk rejected.** The checklist should follow the references and follow the (optional) supplemental material. The checklist does NOT count towards the page limit.

Please read the checklist guidelines carefully for information on how to answer these questions. For each question in the checklist:

- You should answer [Yes], [No], or [NA].
- [NA] means either that the question is Not Applicable for that particular paper or the relevant information is Not Available.
- Please provide a short (1–2 sentence) justification right after your answer (even for NA).

The checklist answers are an integral part of your paper submission. They are visible to the reviewers, area chairs, senior area chairs, and ethics reviewers. You will be asked to also include it (after eventual revisions) with the final version of your paper, and its final version will be published with the paper.

The reviewers of your paper will be asked to use the checklist as one of the factors in their evaluation. While "[Yes]" is generally preferable to "[No]", it is perfectly acceptable to answer "[No]" provided a proper justification is given (e.g., "error bars are not reported because it would be too computationally expensive" or "we were unable to find the license for the dataset we used"). In general, answering "[No]" or "[NA]" is not grounds for rejection. While the questions are phrased in a binary way, we acknowledge that the true answer is often more nuanced, so please just use your best judgment and write a justification to elaborate. All supporting evidence can appear either in the main paper or the supplemental material, provided in appendix. If you answer [Yes] to a question, in the justification please point to the section(s) where related material for the question can be found.

IMPORTANT, please:

- **Delete this instruction block, but keep the section heading “NeurIPS Paper Checklist”,**
- **Keep the checklist subsection headings, questions/answers and guidelines below.**
- **Do not modify the questions and only use the provided macros for your answers.**

1. Claims

Question: Do the main claims made in the abstract and introduction accurately reflect the paper’s contributions and scope?

Answer: [Yes]

Justification: The Abstract and the Introduction include this paper’s contribution and scope.

Guidelines:

- The answer NA means that the abstract and introduction do not include the claims made in the paper.
- The abstract and/or introduction should clearly state the claims made, including the contributions made in the paper and important assumptions and limitations. A No or NA answer to this question will not be perceived well by the reviewers.
- The claims made should match theoretical and experimental results, and reflect how much the results can be expected to generalize to other settings.
- It is fine to include aspirational goals as motivation as long as it is clear that these goals are not attained by the paper.

2. Limitations

Question: Does the paper discuss the limitations of the work performed by the authors?

Answer: [Yes]

Justification: The limitations of our work are discussed in Sec A.

Guidelines:

- The answer NA means that the paper has no limitation while the answer No means that the paper has limitations, but those are not discussed in the paper.
- The authors are encouraged to create a separate "Limitations" section in their paper.
- The paper should point out any strong assumptions and how robust the results are to violations of these assumptions (e.g., independence assumptions, noiseless settings, model well-specification, asymptotic approximations only holding locally). The authors should reflect on how these assumptions might be violated in practice and what the implications would be.
- The authors should reflect on the scope of the claims made, e.g., if the approach was only tested on a few datasets or with a few runs. In general, empirical results often depend on implicit assumptions, which should be articulated.
- The authors should reflect on the factors that influence the performance of the approach. For example, a facial recognition algorithm may perform poorly when image resolution is low or images are taken in low lighting. Or a speech-to-text system might not be used reliably to provide closed captions for online lectures because it fails to handle technical jargon.
- The authors should discuss the computational efficiency of the proposed algorithms and how they scale with dataset size.
- If applicable, the authors should discuss possible limitations of their approach to address problems of privacy and fairness.
- While the authors might fear that complete honesty about limitations might be used by reviewers as grounds for rejection, a worse outcome might be that reviewers discover limitations that aren't acknowledged in the paper. The authors should use their best judgment and recognize that individual actions in favor of transparency play an important role in developing norms that preserve the integrity of the community. Reviewers will be specifically instructed to not penalize honesty concerning limitations.

3. Theory assumptions and proofs

Question: For each theoretical result, does the paper provide the full set of assumptions and a complete (and correct) proof?

Answer: [\[Yes\]](#)

Justification: We ensure the correctness of loss derivation in Sec 3. The equivalence of the gradient constraint in Eq 3 and the Lipchitz condition that SNR ensures is provided in Sec C in Appendix.

Guidelines:

- The answer NA means that the paper does not include theoretical results.
- All the theorems, formulas, and proofs in the paper should be numbered and cross-referenced.
- All assumptions should be clearly stated or referenced in the statement of any theorems.
- The proofs can either appear in the main paper or the supplemental material, but if they appear in the supplemental material, the authors are encouraged to provide a short proof sketch to provide intuition.
- Inversely, any informal proof provided in the core of the paper should be complemented by formal proofs provided in appendix or supplemental material.
- Theorems and Lemmas that the proof relies upon should be properly referenced.

4. Experimental result reproducibility

Question: Does the paper fully disclose all the information needed to reproduce the main experimental results of the paper to the extent that it affects the main claims and/or conclusions of the paper (regardless of whether the code and data are provided or not)?

Answer: [Yes]

Justification: We provided guidelines for reproducing our experiment in Sec G.3 in Appendix.

Guidelines:

- The answer NA means that the paper does not include experiments.
- If the paper includes experiments, a No answer to this question will not be perceived well by the reviewers: Making the paper reproducible is important, regardless of whether the code and data are provided or not.
- If the contribution is a dataset and/or model, the authors should describe the steps taken to make their results reproducible or verifiable.
- Depending on the contribution, reproducibility can be accomplished in various ways. For example, if the contribution is a novel architecture, describing the architecture fully might suffice, or if the contribution is a specific model and empirical evaluation, it may be necessary to either make it possible for others to replicate the model with the same dataset, or provide access to the model. In general, releasing code and data is often one good way to accomplish this, but reproducibility can also be provided via detailed instructions for how to replicate the results, access to a hosted model (e.g., in the case of a large language model), releasing of a model checkpoint, or other means that are appropriate to the research performed.
- While NeurIPS does not require releasing code, the conference does require all submissions to provide some reasonable avenue for reproducibility, which may depend on the nature of the contribution. For example
 - (a) If the contribution is primarily a new algorithm, the paper should make it clear how to reproduce that algorithm.
 - (b) If the contribution is primarily a new model architecture, the paper should describe the architecture clearly and fully.
 - (c) If the contribution is a new model (e.g., a large language model), then there should either be a way to access this model for reproducing the results or a way to reproduce the model (e.g., with an open-source dataset or instructions for how to construct the dataset).
 - (d) We recognize that reproducibility may be tricky in some cases, in which case authors are welcome to describe the particular way they provide for reproducibility. In the case of closed-source models, it may be that access to the model is limited in some way (e.g., to registered users), but it should be possible for other researchers to have some path to reproducing or verifying the results.

5. Open access to data and code

Question: Does the paper provide open access to the data and code, with sufficient instructions to faithfully reproduce the main experimental results, as described in supplemental material?

Answer: [Yes]

Justification: We provide open access to our code in the anonymous link . We will make the code publicly accessible upon acceptance.

Guidelines:

- The answer NA means that paper does not include experiments requiring code.
- Please see the NeurIPS code and data submission guidelines (<https://nips.cc/public/guides/CodeSubmissionPolicy>) for more details.

- While we encourage the release of code and data, we understand that this might not be possible, so “No” is an acceptable answer. Papers cannot be rejected simply for not including code, unless this is central to the contribution (e.g., for a new open-source benchmark).
- The instructions should contain the exact command and environment needed to run to reproduce the results. See the NeurIPS code and data submission guidelines (<https://nips.cc/public/guides/CodeSubmissionPolicy>) for more details.
- The authors should provide instructions on data access and preparation, including how to access the raw data, preprocessed data, intermediate data, and generated data, etc.
- The authors should provide scripts to reproduce all experimental results for the new proposed method and baselines. If only a subset of experiments are reproducible, they should state which ones are omitted from the script and why.
- At submission time, to preserve anonymity, the authors should release anonymized versions (if applicable).
- Providing as much information as possible in supplemental material (appended to the paper) is recommended, but including URLs to data and code is permitted.

6. Experimental setting/details

Question: Does the paper specify all the training and test details (e.g., data splits, hyper-parameters, how they were chosen, type of optimizer, etc.) necessary to understand the results?

Answer: [Yes]

Justification: We have provided the experiment details in Sec G in Appendix.

Guidelines:

- The answer NA means that the paper does not include experiments.
- The experimental setting should be presented in the core of the paper to a level of detail that is necessary to appreciate the results and make sense of them.
- The full details can be provided either with the code, in appendix, or as supplemental material.

7. Experiment statistical significance

Question: Does the paper report error bars suitably and correctly defined or other appropriate information about the statistical significance of the experiments?

Answer: [No]

Justification: We have not reported error bars like previous works. We believe this is acceptable because the relative improvement of our method is significantly beyond the statistical error. For experiments requiring statistical verification, we provided the box plot in Fig 18 where deviation is considered.

Guidelines:

- The answer NA means that the paper does not include experiments.
- The authors should answer "Yes" if the results are accompanied by error bars, confidence intervals, or statistical significance tests, at least for the experiments that support the main claims of the paper.
- The factors of variability that the error bars are capturing should be clearly stated (for example, train/test split, initialization, random drawing of some parameter, or overall run with given experimental conditions).
- The method for calculating the error bars should be explained (closed form formula, call to a library function, bootstrap, etc.)
- The assumptions made should be given (e.g., Normally distributed errors).

- It should be clear whether the error bar is the standard deviation or the standard error of the mean.
- It is OK to report 1-sigma error bars, but one should state it. The authors should preferably report a 2-sigma error bar than state that they have a 96% CI, if the hypothesis of Normality of errors is not verified.
- For asymmetric distributions, the authors should be careful not to show in tables or figures symmetric error bars that would yield results that are out of range (e.g. negative error rates).
- If error bars are reported in tables or plots, The authors should explain in the text how they were calculated and reference the corresponding figures or tables in the text.

8. Experiments compute resources

Question: For each experiment, does the paper provide sufficient information on the computer resources (type of compute workers, memory, time of execution) needed to reproduce the experiments?

Answer: [Yes]

Justification: The hardware information is listed in Sec G. We also include Sec G.4 on efficiency in the Appendix. Only the training costs are discussed since our method does not introduce any additional cost in inference (actual deployment).

Guidelines:

- The answer NA means that the paper does not include experiments.
- The paper should indicate the type of compute workers CPU or GPU, internal cluster, or cloud provider, including relevant memory and storage.
- The paper should provide the amount of compute required for each of the individual experimental runs as well as estimate the total compute.
- The paper should disclose whether the full research project required more compute than the experiments reported in the paper (e.g., preliminary or failed experiments that didn't make it into the paper).

9. Code of ethics

Question: Does the research conducted in the paper conform, in every respect, with the NeurIPS Code of Ethics <https://neurips.cc/public/EthicsGuidelines>?

Answer: [Yes]

Justification: Yes, we follow the Code of Ethics.

Guidelines:

- The answer NA means that the authors have not reviewed the NeurIPS Code of Ethics.
- If the authors answer No, they should explain the special circumstances that require a deviation from the Code of Ethics.
- The authors should make sure to preserve anonymity (e.g., if there is a special consideration due to laws or regulations in their jurisdiction).

10. Broader impacts

Question: Does the paper discuss both potential positive societal impacts and negative societal impacts of the work performed?

Answer: [NA]

Justification: While our work may have various societal implications, we believe none are significant enough to warrant specific mention here.

Guidelines:

- The answer NA means that there is no societal impact of the work performed.

- If the authors answer NA or No, they should explain why their work has no societal impact or why the paper does not address societal impact.
- Examples of negative societal impacts include potential malicious or unintended uses (e.g., disinformation, generating fake profiles, surveillance), fairness considerations (e.g., deployment of technologies that could make decisions that unfairly impact specific groups), privacy considerations, and security considerations.
- The conference expects that many papers will be foundational research and not tied to particular applications, let alone deployments. However, if there is a direct path to any negative applications, the authors should point it out. For example, it is legitimate to point out that an improvement in the quality of generative models could be used to generate deepfakes for disinformation. On the other hand, it is not needed to point out that a generic algorithm for optimizing neural networks could enable people to train models that generate Deepfakes faster.
- The authors should consider possible harms that could arise when the technology is being used as intended and functioning correctly, harms that could arise when the technology is being used as intended but gives incorrect results, and harms following from (intentional or unintentional) misuse of the technology.
- If there are negative societal impacts, the authors could also discuss possible mitigation strategies (e.g., gated release of models, providing defenses in addition to attacks, mechanisms for monitoring misuse, mechanisms to monitor how a system learns from feedback over time, improving the efficiency and accessibility of ML).

11. Safeguards

Question: Does the paper describe safeguards that have been put in place for responsible release of data or models that have a high risk for misuse (e.g., pretrained language models, image generators, or scraped datasets)?

Answer: [NA]

Justification: This paper poses no such risks.

Guidelines:

- The answer NA means that the paper poses no such risks.
- Released models that have a high risk for misuse or dual-use should be released with necessary safeguards to allow for controlled use of the model, for example by requiring that users adhere to usage guidelines or restrictions to access the model or implementing safety filters.
- Datasets that have been scraped from the Internet could pose safety risks. The authors should describe how they avoided releasing unsafe images.
- We recognize that providing effective safeguards is challenging, and many papers do not require this, but we encourage authors to take this into account and make a best faith effort.

12. Licenses for existing assets

Question: Are the creators or original owners of assets (e.g., code, data, models), used in the paper, properly credited and are the license and terms of use explicitly mentioned and properly respected?

Answer: [Yes]

Justification: The code and datasets used in the paper are publicly available and properly credited.

Guidelines:

- The answer NA means that the paper does not use existing assets.
- The authors should cite the original paper that produced the code package or dataset.

- The authors should state which version of the asset is used and, if possible, include a URL.
- The name of the license (e.g., CC-BY 4.0) should be included for each asset.
- For scraped data from a particular source (e.g., website), the copyright and terms of service of that source should be provided.
- If assets are released, the license, copyright information, and terms of use in the package should be provided. For popular datasets, paperswithcode.com/datasets has curated licenses for some datasets. Their licensing guide can help determine the license of a dataset.
- For existing datasets that are re-packaged, both the original license and the license of the derived asset (if it has changed) should be provided.
- If this information is not available online, the authors are encouraged to reach out to the asset's creators.

13. **New assets**

Question: Are new assets introduced in the paper well documented and is the documentation provided alongside the assets?

Answer: [\[Yes\]](#)

Justification: We will make the code publicly available upon acceptance of the paper and provide detailed documentation

Guidelines:

- The answer NA means that the paper does not release new assets.
- Researchers should communicate the details of the dataset/code/model as part of their submissions via structured templates. This includes details about training, license, limitations, etc.
- The paper should discuss whether and how consent was obtained from people whose asset is used.
- At submission time, remember to anonymize your assets (if applicable). You can either create an anonymized URL or include an anonymized zip file.

14. **Crowdsourcing and research with human subjects**

Question: For crowdsourcing experiments and research with human subjects, does the paper include the full text of instructions given to participants and screenshots, if applicable, as well as details about compensation (if any)?

Answer: [\[NA\]](#)

Justification: This work does not involve crowdsourcing nor research with human subjects.

Guidelines:

- The answer NA means that the paper does not involve crowdsourcing nor research with human subjects.
- Including this information in the supplemental material is fine, but if the main contribution of the paper involves human subjects, then as much detail as possible should be included in the main paper.
- According to the NeurIPS Code of Ethics, workers involved in data collection, curation, or other labor should be paid at least the minimum wage in the country of the data collector.

15. **Institutional review board (IRB) approvals or equivalent for research with human subjects**

Question: Does the paper describe potential risks incurred by study participants, whether such risks were disclosed to the subjects, and whether Institutional Review Board (IRB)

approvals (or an equivalent approval/review based on the requirements of your country or institution) were obtained?

Answer: [NA]

Justification: This work does not involve crowdsourcing nor research with human subjects.

Guidelines:

- The answer NA means that the paper does not involve crowdsourcing nor research with human subjects.
- Depending on the country in which research is conducted, IRB approval (or equivalent) may be required for any human subjects research. If you obtained IRB approval, you should clearly state this in the paper.
- We recognize that the procedures for this may vary significantly between institutions and locations, and we expect authors to adhere to the NeurIPS Code of Ethics and the guidelines for their institution.
- For initial submissions, do not include any information that would break anonymity (if applicable), such as the institution conducting the review.

16. Declaration of LLM usage

Question: Does the paper describe the usage of LLMs if it is an important, original, or non-standard component of the core methods in this research? Note that if the LLM is used only for writing, editing, or formatting purposes and does not impact the core methodology, scientific rigorousness, or originality of the research, declaration is not required.

Answer: [NA]

Justification: The core method development of this work does not involve LLM.

Guidelines:

- The answer NA means that the core method development in this research does not involve LLMs as any important, original, or non-standard components.
- Please refer to our LLM policy (<https://neurips.cc/Conferences/2025/LLM>) for what should or should not be described.